Sensing Behavior of Galfenol (FeGa) Alloys under Dynamic Conditions

Undergraduate Honors Thesis

Presented in Partial Fulfillment of the Requirements for

Graduation with Distinction

at The Ohio State University

By

Travis Walker

****

The Ohio State University

2011

Approved By:

Defense Committee:

Professor Marcelo Dapino, Advisor

Professor Yann Guezennec

_____

Advisor
Graduate Program in
Mechanical Engineering

ABSTRACT

Magnetostrictive materials are a class of smart materials that have the capability to convert mechanical energy to magnetic energy and vice versa. This material property makes these materials ideal for both sensing and actuation applications. Utilizing a customized part composed of only one material, rather than various components working together, would lessen the effect of wear and degradation in addition to allowing the customized part to be much smaller than current counterparts. These devices can be self contained, and in some cases can be used as self-sensing actuators. Galfenol, an alloy of iron and gallium, is a promising material for such application due to the moderate strain exhibited under a magnetic field combined with the material's mechanical robustness.

This research looks to further the study of Galfenol by documenting the behavior of ($Fe_{81.6}Ga_{18.4}$) Galfenol in the dynamic (time-varying) regime in relation to sensing applications. The characterization of these alloys involves applying a dynamic stress to the sample and measuring the corresponding change in magnetization level. Using an array of different probes and sensors these results have been obtained for different frequencies of stress excitation. The relationship between the input stress and the output magnetization is non-linear and exhibits hysteresis. The characterization of these responses aids in the creation of guidelines for implementing Galfenol in a sensing or actuating system.

ACKNOWLEDGMENTS

I would like to thank everyone who has helped me along the way. First, I would like to thank my advisor, Dr. Marcelo Dapino, for his guidance and advice through the process of this research. Next, I would like to thank all of the other students in the Smart Materials and Structures Laboratory, especially Arjun Mahadevan. Their help with procedures and equipment was invaluable to this project. I would also like to aknowledge the Department of Mechanical Engineering at The Ohio State Univeristy. The facilities in the department were a great asset in completing this research. I would like to thank family and friends. My friends have provided me with various forms of support through encouragement or even distractions when neccessary. My family has played a large role in allowing me to reach the point where I currently am. I would especially like to thank my parents for all that they have done in my life. Their love and encouragement have helped me to stay focused, while their example of hard work ethic and perserverance have given me a goal to strive for.

TABLE OF CONTENTS

Page

LIST OF FIGURES

Figure Page

CHAPTER 1

INTRODUCTION

1.1 Background

Sensing and actuation are two important aspects of engineering that are constantly being studied and applied to new and evolving technologies. These two areas are important to many industries because of the ability to measure and determine the forces and other effects acting on a system, as well as using that information to control the response of these systems. Today's modern technology has been studied and improved through many years of research; however, there are still limitations with the current methods of sensing and actuation. These shortcomings have led to the industry's interest in smart materials. These materials have special properties caused from the interaction between different conditions. The study of smart materials is of increasing interest in the area of technology because of the possible benefits to different critical areas of science including aerospace, automotive, and even medical solutions.

Smart materials are a special set of materials that change in some way as a response to a change in their environment. A change in temperature,

electric field, magnetic field or some other external stimuli causes a change in the smart material. This change is documented in a controlled manner, and by understanding the relationship between the change in the material and the change in the environment, these materials can be used to convert one form of energy to another. This transformation of energy has made smart materials an excellent selection for actuating and sensing devices. There has been extensive research into the study of Shape Memory Alloys (SMA's) and piezoelectric materials. SMA's are used in high strain and low frequency operations while piezoelectric materials are better suited for low strain and high frequency operations. SMA's typically take advantage of a change in temperature whereas piezoelectric materials exhibit a relationship with the electric field. [1]

Magnetostrictive materials are a type of smart materials that exhibit a coupling of magnetic energy to mechanical energy and vice versa. These materials have the ability to deform their shape with a change in magnetic field as well as producing a magnetic field with the application of a stress. The strain caused by the magnetic field, magnetostriction, is what gives these materials their name. This coupling allows for one part of a system to serve multiple functions which provides for more compact and durable systems. These multi-function systems have potential benefits in not only industry, but also in medical and defense applications. Making use of the actuation characteristics of magnetostrictive materials could lead to developments in vibration control, sonar transducers, and micropositioners. Potential uses of

the sensing characteristics are non-contact torque sensors, wave guide position sensors, and acoustic sensors. [3]

The history of magnetostrictive materials began in the early 1840's with the discovery by James P. Joule that a sample of iron changed length as it was magnetized. This discovery led to the research of magnetostriction in materials such as nickel, iron, and other ferromagnetic materials. These materials exhibit strains on the order of 10 x 10^{-6} and were first used in telephone receivers, hydrophones, torque-meters, and scanning sonar. [5] In the 1970's the study of magnetostrictive materials received more attention because of the discovery of "giant" magnetostrictive materials. By adding rare earth ions such as terbium (Tb) and dysprosium (Dy) to an iron sample, the magnetostriction was on the order of 1000 x 10^{-6}. Taking advantage of this knowledge, the Naval Ordnance Laboratory began creating $Tb_{0.3}Dy_{0.7}Fe_{1.9-1.95}$. This material known as Terfenol-D (terbium: Ter; iron: Fe; Naval Ordnance Laboratory: NOL; dysporosium: D) exhibits a saturation magnetostriction of 1,600 x 10^{-6} under a moderate saturation field of 160 kA/m and has been commercially available since the 1980's. [4] The large amount of magnetostriction makes these rare-earth alloys an interesting area of study; however, their brittle nature limits their use in many applications. This limitation has led to the investigation of new magnetostrictive materials that have superior mechanical durability.

This search has led to the creation of Galfenol alloys ($Fe_{1-x}Ga_x$) or iron-gallium alloys where the value of percent of gallium varies between 12 and

29%. Galfenol was also discovered by the Naval Ordnance Laboratory and has superior mechanical properties to the rare-earth ion alloys. These alloys exhibit moderate magnetostriction at low saturation fields, and have a mechanical robustness similar to steel. This means that Galfenol alloys can accommodate tensile, compressive, bending, and torque loading. The metallurgical properties also allows for Galfenol to be machined, welded, extruded, and deposited into complex geometries. The unique combination of mechanical robustness and moderate magnetostriction gives Galfenol the opportunity to be used as shock-tolerant adaptive structures, nanoacoustic sensors that mimic the cilia of the inner ear, as well as sonar transducers with load bearing capabilities. [9] Galfenol is a promising alloy for use in sensors and actuators; however, due to its relatively recent discovery there is still much work that needs to be done to better understand its behavior.

1.2 Literature Review

1.2.1 Principles of Magnetostriction

Magnetostrictive materials couple the magnetic and mechanical domains, in other words, there exists a relationship between the magnetic properties of these materials with their mechanical properties. The following illustrations show how the actuating and sensing effects work. One can also see how the rotation of the magnetic domains is one of the important characteristics of magnetostrictive materials.

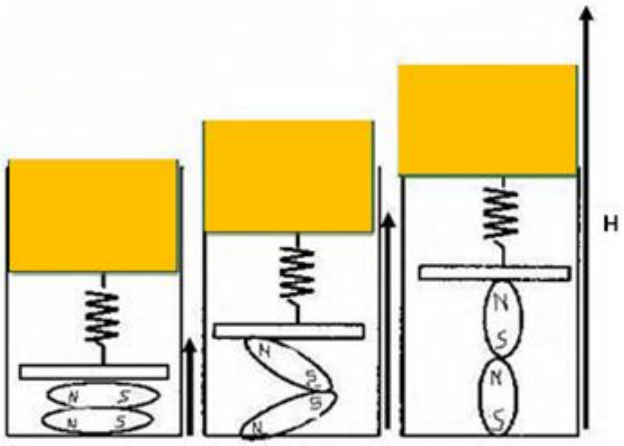

Figure 1.1: Magnetostrictive Actuation with
Constant Stress **T** and Increasing Magnetic Field **H** [1]

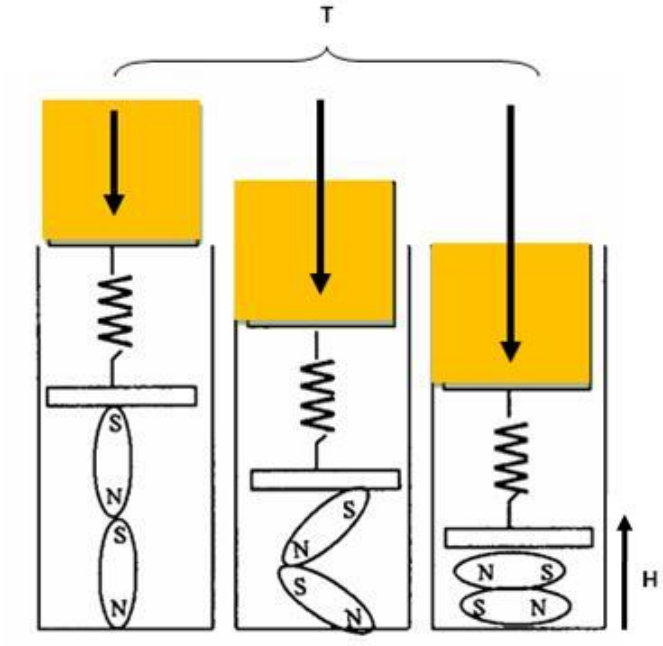

Figure 1.2: Magnetostrictive Sensing with
Constant Magnetic Field **H** and Increasing Stress **T** [1]

For magnetostrictive materials, the Magnetization $\mathbf{M}$, or $B = \mu_0(H+M)$, and strain $\mathbf{S}$ respond to changes in magnetic field $\mathbf{H}$ and stress $\mathbf{T}$ in a nonlinear manner that depends on the material history. The two components of the nonlinearity are saturation and anisotropy. Saturation occurs in both the magnetization and the magnetostriction. These materials are also directionally dependent and anisotropic so they have a different response in one crystal direction as compared to another direction.

To account for this nonlinear behavior, sensors and actuators are generally designed for small operating ranges around a particular bias field or stress. Under these conditions, the constitutive behavior can be modeled by,

$$B = \mu^T H + dT, \tag{1.1}$$

$$S = d^T H + s^H T. \tag{1.2}$$

These equations make use of the coupling coefficients: the permeability tensor μ^T (measured at constant stress), the compliance tensor $\mathbf{s}^H$ (measured at constant field), and the piezomagnetic tensor $\mathbf{d}$. The piezomagnetic tensor $\mathbf{d}$ determines the maximum free strain when $\mathbf{T} = 0$. The free strain is $\mathbf{d}^T\mathbf{H}$. The piezomagnetic tensor and the compliance tensor together determine the maximum possible stress, or blocked stress, when $\mathbf{S} = 0$. This stress is $(\mathbf{s}^H)^{-1}\mathbf{dH}$.

The energy density or work capacity is given as half the product of the free strain and the blocked stress. The free energy $\mathbf{G}$ is then shown by,

$$G = \frac{1}{2}(T \cdot S + H \cdot B) \tag{1.3}$$

$$= \frac{1}{2}T \cdot s^H T + \frac{1}{2}(T \cdot d^T H + H \cdot dT) + \frac{1}{2}H \cdot \mu^T H \tag{1.4}$$

$$= G_{mechanical} + 2G_{coupling} + G_{magnetic}. \tag{1.5}$$

The coupling coefficient k for these materials is given by,

$$k = \frac{G_{coupling}}{\sqrt{G_{mechanical}G_{magnetic}}}, \tag{1.6}$$

$$k = \frac{d^2}{s^H \mu^T}. \tag{1.7}$$

These coupling equations define the behavior for magnetostrictive materials, therefore the corresponding coupling coefficients are important material properties in the design of magnetostrictive devices. [1],[8]

1.2.2 Static Galfenol

Much of the previous work done in the research of Galfenol has been based on static determination of material characteristics. These studies have looked at different aspects of Galfenol especially regarding how the amount of gallium in a sample affects the material properties. One area of particular interest is in the amount of magnetostriction obtainable as determined by the gallium content.

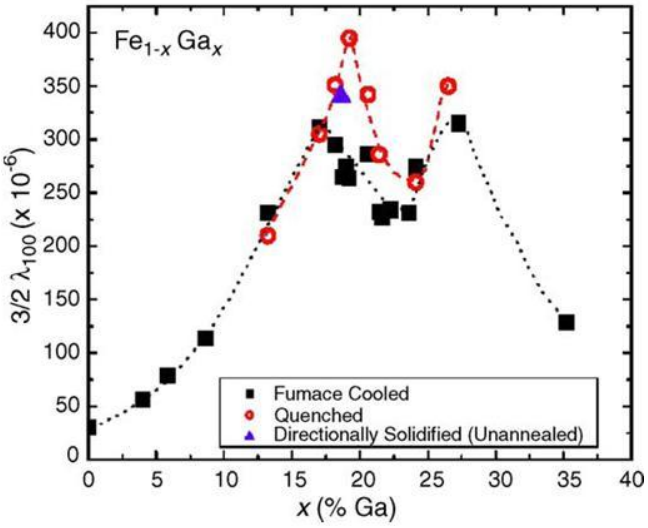

Figure 1.3: Magnetostriction for Different Compositions of at.% Ga [7]

Figure 1.3 shows that the magnetostriction of Galfenol has a maximum response at 17 at.% Ga for furnace cooled samples and 19 at.% Ga for quenched samples. For this reason, much of the subsequent research on Galfenol has been done with samples near this peak. The next area of interest in the study of Galfenol was to look at how a sample responded under different stresses and fields. Much of this research was performed in the quasi-static regime.

1.2.3 Quasi-Static Galfenol

Galfenol has been tested extensively under quasi-static operating conditions for both sensing and actuation characteristics. These studies were used to better understand the non-linearity and hysteretic behavior of the material. In a study performed by Kellogg et al. both single crystal and

polycrystalline samples of $Fe_{81}Ga_{19}$ were tested under constant temperature varying from -21°C to 80°C. The results showed that the response of Galfenol was temperature insensitive with a small 12% variation in maximum magnetostriction and a 3.6% variation in maximum magnetization. The magnetostriction decreased from 340 x 10^{-6} to 298 x 10^{-6} while the magnetization decreased from 1313 kA/m to 1265 kA/m. This study also showed that the field necessary for saturation of the sample increased as the compressive stress increased and the hysteretic losses observed in Galfenol were significantly smaller than those observed in Terfenol-D. In comparing the polycrystalline samples with the single crystal samples, the saturation magnetization was higher for the polycrystalline samples while the magnetostriction was lower. [13]

Further study on the effects of stress and field on magnetization and magnetostriction was completed by Mahadaven. The actuation and sensing characteristics for both $Fe_{81.6}Ga_{18.4}$ and $Fe_{79.1}Ga_{20.9}$ samples were tested. The actuation characteristics were obtained by applying a constant stress and varying the field. The sensing tests were completed by applying a constant field and varying the stress. The results for the $Fe_{81.6}Ga_{18.4}$ sample are shown below in Figure 1.4. These results agree with the findings by Kellogg et al. and show that there is very little change in magnetization or magnetostriction under tensile loading. This is because tensile loading pre-aligns the magnetic domains along the axis of the rod which causes very little change in dimension of the sample with an applied field along the axis of the rod. [15]

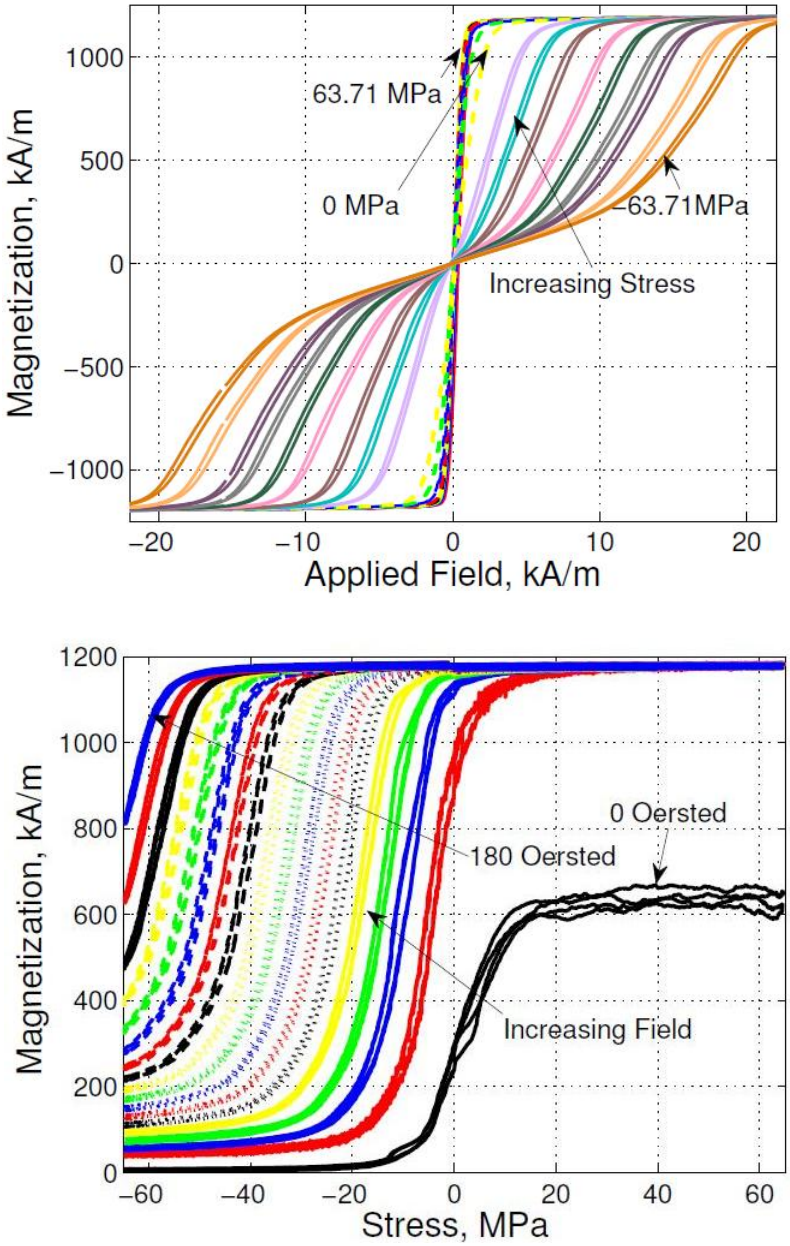

Figure 1.4: Magnetization Loops for $Fe_{81.6}Ga_{18.4}$ for (Top) applied field with different constant stresses and (Bottom) applied stress with different constant fields [15]

In addition to experimental results, Evans and Dapino have developed a constitutive model relating magnetization and strain to magnetic field and stress. In addition to this model, they created a model to characterize the stress dependent susceptibility of Galfenol and the potential use in a force sensor application. This model uses the domain rotation of a Galfenol sample as the primary means of magnetization. Figure 1.5 shows a force sensor schematic that would use an excitation voltage to create a flux in the sample, and then measure the changing pickup coil voltage as it changes with the applied load. The model developed by Evans and Dapino show that $Fe_{79.1}Ga_{20.9}$ has a higher susceptibility than $Fe_{81.6}Ga_{18.4}$. [11]

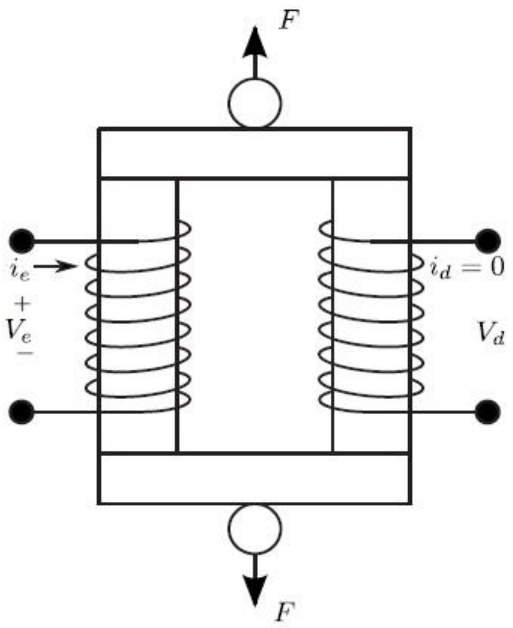

Figure 1.5: Force Sensing Transducer with Magnetostrictive Core [11]

The force sensor described above makes use of a signal modulation scheme to capture the data. In this process, the field is excited sinusoidally at a frequency much higher than the frequency of the stress excitation. The modulation technique allows for the sensor to be operated around the zero field level, because with a constant current to the coils of zero amperes there is very little change in the magnetization of the sample. Signal modulation is created when two sinusoidal waves are superimposed together through multiplication. A demodulation scheme is then applied to recover the low frequency signal. This process will be discussed further in Chapter 3.

1.2.4 Dynamic Galfenol

There has currently been little work in the study of Galfenol under dynamic operating conditions. Poeppelman has expanded the knowledge base for the dynamic characterization of Galfenol with his study of the actuation behavior of Galfenol. By causing a sinusoidal magnetic field through the Galfenol sample at varying frequencies up to 500 Hz, the variation in magnetization and strain with respect to frequency was determined. The results of these experiments showed an increase in the hysteresis loss experienced by the Galfenol sample as the frequency of the magnetic field was increased. There was also an increase in phase at higher frequencies. [17]

1.3 Motivation

The literature review provides a basis for understanding Galfenol in the static regime, but due to the large number of potential applications in the dynamic regime there is still more work to be done to fully understand the behavior of this material. The work described in this thesis will focus on the dynamic behavior of Galfenol, especially with respect to sensing applications. This research is funded by the MURI grant through the Office of Naval Research as well as MOOG, Inc. The results will be used in conjunction with the results described in the literature review to fully understand the response of Galfenol. This information will be important in controlling Galfenol devices as well as using Galfenol to sense and control other systems.

1.4 Project Objectives

This project was originated to increase the understanding of Galfenol under dynamic operating conditions. A proper testing procedure and apparatus were designed to apply a force to the Galfenol sample, and the subsequent response observed using a number of sensors. An appropriate data acquisition plan was developed to record the observed response. The test procedure was validated by comparing results obtained under quasi-static conditions with the results mentioned in the literature review. After validating the testing procedure, dynamic tests were conducted by subjecting the Galfenol sample to a sinusoidally varying force. The response was observed and the results

analyzed to further characterize Galfenol under dynamic conditions.

This research is also designed to further the development of a dynamic force sensor using magnetostrictive Galfenol alloys. The results of this research will be used in conjunction with the previous results to create guidelines for creating a force sensor using Galfenol. The work described in this thesis looks at the sensing characteristics of Galfenol alloys, and how that can be implemented into a real world sensor.

CHAPTER 2

TEST SET-UP

This chapter will discuss the different components used in the testing process conducted as a part of this thesis. The testing was designed to focus on the sensing characteristics of a sample of a research grade, highly textured, <100> orientated polycrystalline Galfenol alloy with a composition of $Fe_{81.6}Ga_{18.4}$. The test set up was designed for dynamic tests to further expand the knowledge base for Galfenol alloys in the dynamic operating region.

2.1 Overview

This work was designed to document and observe the sensing characteristics of Galfenol alloys under dynamic loading conditions. To accomplish this task, a sinusoidally varying load was required to be applied along the axial direction of a rod while a constant magnetic field was applied through the sample. As the load was applied several quantities needed to be measured which included: the applied force, strain in the rod, magnetic flux density in the rod, and magnetic field on the rod surface. These required measure-

ments created a need for multiple sensors and other measurements that were integrated into the test set-up. Figure 2.1 shows the test set-up used in the experiments described later in this thesis. The following sections describe in more detail the different components used in the testing process.

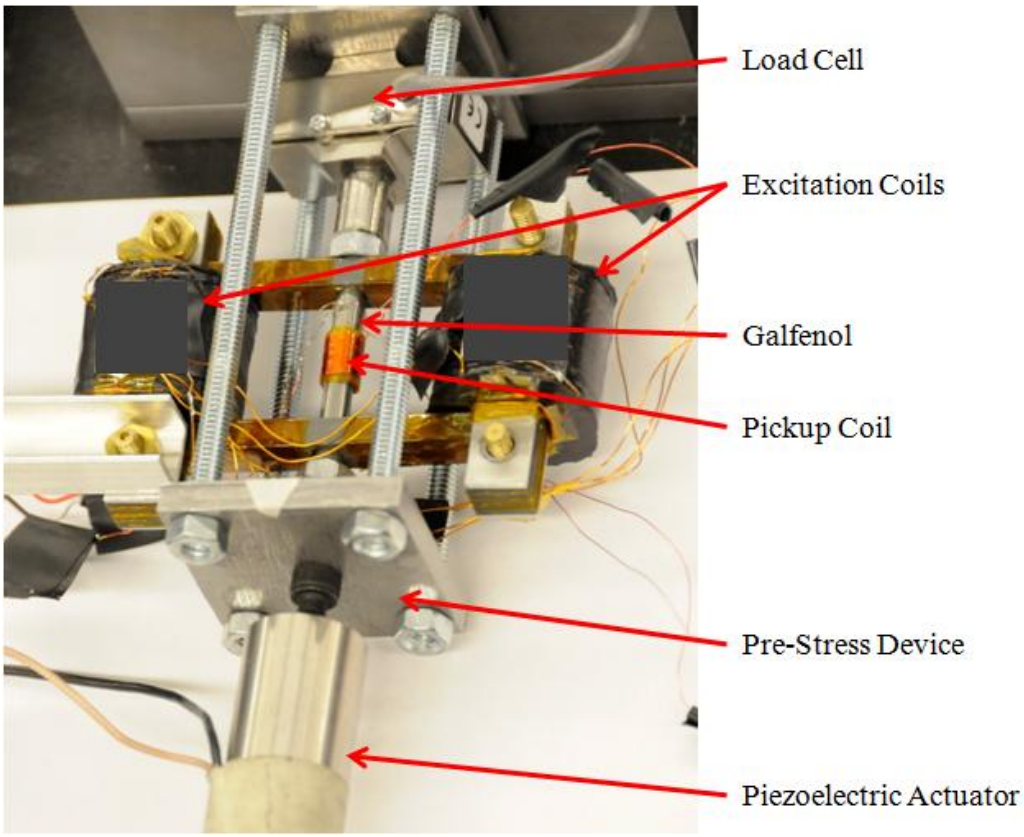

Figure 2.1: Testing Apparatus with Different Components Labeled

2.2 Force Generation

The generation of a force on the sample is the key component to obtaining sensing characteristics for Galfenol alloys. The requirement of the applied

force being sinusoidal and at varying frequencies added additional necessary specifications to the device used to generate this force. There are many ways to apply a force to a sample including: free weights, hydraulic actuators, piezoelectric actuators, and magnetostrictive actuators. Due to the desire for high frequency load applications, the free weights and hydraulic actuators were eliminated from further considerations. Free weights are used in static testing, and while hydraulic actuators can be used in low frequency applications, their response time is not quick enough for high frequencies.

The remaining two categories were considered, and a piezoelectric actuator was selected because of the linear relationship between input voltage and output displacement. Magnetostrictive actuators have a non-linear behavior which would prove more difficult to control and skew the results of testing on Galfenol, another magnetostrictive material. For these reasons a PSt 1000/16/80 VS25 piezoelectric actuator from American Piezo, LTD was chosen. This actuator was controlled through a high voltage input. As the voltage is increased the actuator displaces and if this displacement is prevented a force is generated. The use of this theory is described in the next section. Figure 2.2 shows the actuator which is a stack of several piezoelectric elements encased in a steel casing which applies a pre-stress to the stack. This pre-stress helps to prevent tensile loading on the stack which would lead to failure.

Figure 2.2: PSt 1000/16/80 VS25 Piezoelectric Actuator from American Piezo, LTD

2.3 Block Test

The force generated by the actuator is due to the fact that the displacement caused by the input voltage is blocked or prevented. The actuator chosen for these experiments has a maximum displacement of 80 μm. To achieve high forces on the sample, the displacement of each component in the path of the force must be minimized. This is to say that the load cell, the supports, the couplers, and any other components used in the connection process should be stiffer than the Galfenol sample. The frame design was the area of concern in the construction of this apparatus. To determime the stiffness of the frame design, it was modeled in a finite element program called COMSOL. Figure 2.3 shows the frame as modeled in COMSOL.

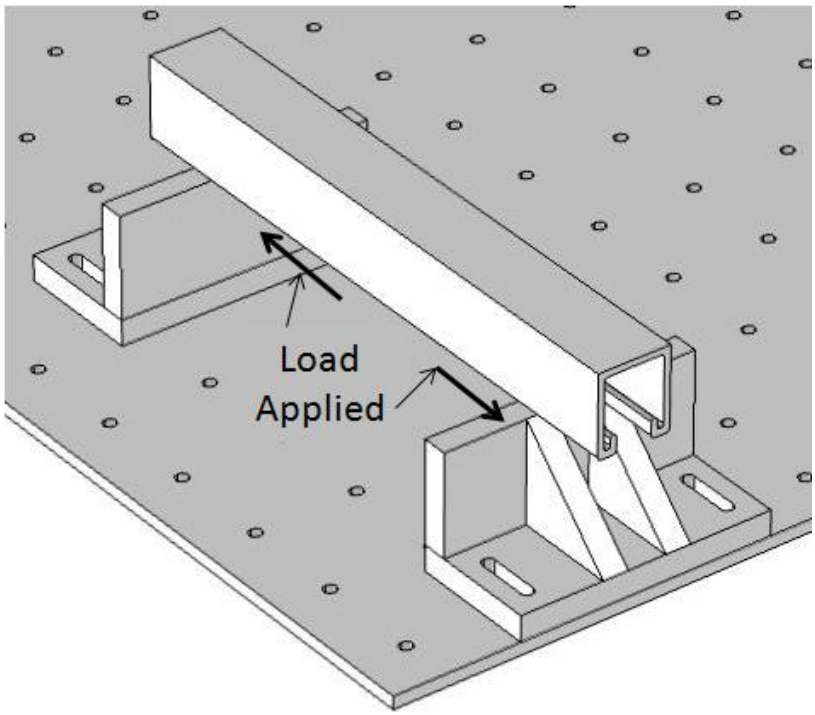

Figure 2.3: COMSOL Model of Frame Structure

The frame subjected to a static 1335 N force and the resulting deflection recorded. From this data it was determined that the frame structure made of half inch steel with a crossbar. The final design for the supports provided a stiffness of 1.07 x 10^9 N/m which is approximately 26 times stiffer than the Galfenol sample. The actuator, Galfenol sample, and load cell were placed between the two support structures. Also to further improve the stiffness of the set-up, a crossbar was added to effectively make the set up a frame. With the supports screwed to the base and the crossbar connecting the tops of the supports there is very little displacement in the frame as the force is applied from the actuator. The crossbar also had the added benefit of providing a

mounting location for a sensor. Figure 2.4 depicts the support structure in use.

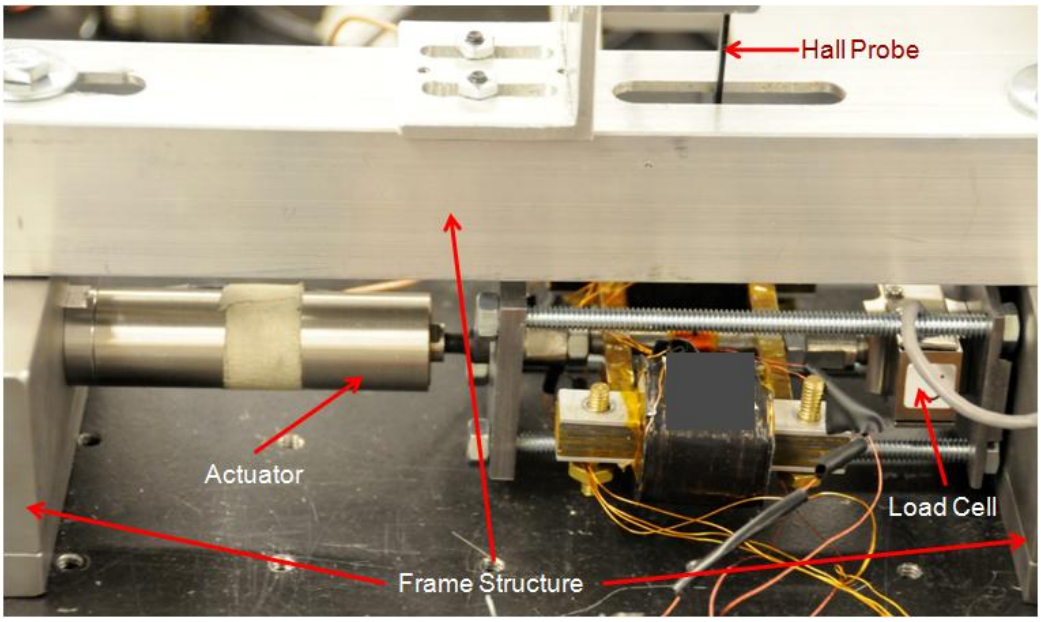

Figure 2.4: Block Test Frame

2.4 Magnetic Flux Circuit

Being that Galfenol is a magnetostrictive material, the values of merit are magnetic flux density and magnetic field. For sensing characteristics of Galfenol the magnetic field is held constant while the force is applied and the magnetic flux density is observed. This flux density is then used to calculate the corresponding magnetization of the Galfenol sample.

For the experiments run as part of this thesis, the magnetic flux circuit as shown in Figure 2.5 was used.[17] This magnetic flux circuit consists of

two excitation coils that when supplied with a current produce a magnetic flux inside each coil. The flux then travels through the structure of the magnetic flux circuit so as to enter the Galfenol sample. The structure of the flux circuit is made of steel laminates to reduce the effect of eddy currents. The flux through the Galfenol creates a magnetic field on the surface of the sample. The current through the excitation coils can be adjusted to create the different levels of magnetic field present in the experiments described in this thesis.

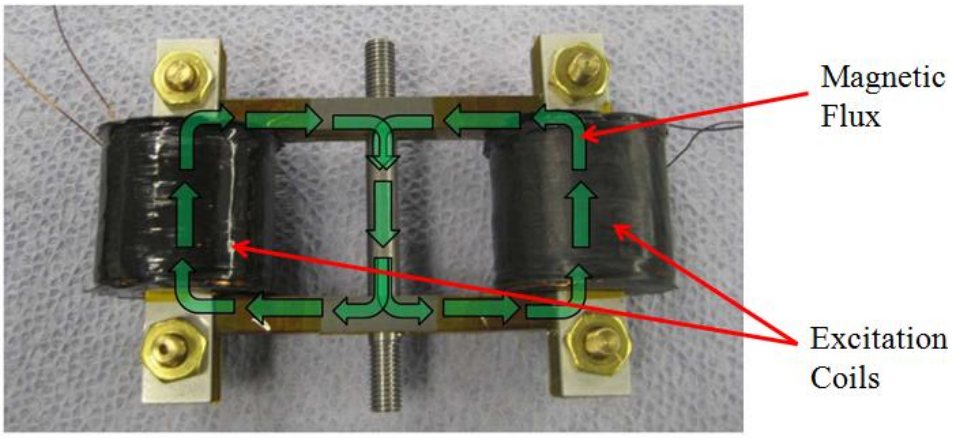

Figure 2.5: Magnetic Flux Circuit

2.5 Pre-Stress

Pre-stressing Galfenol alloys is one way to improve the magnetostriction effects during actuation. In sensing, the effect of pre-stress has a slightly different benefit. As the magnetic field is applied to the sample, the magnetic domains align themselves along the axis of the rod in the direction of the

field causing saturation. There is no change in magnetization when a tensile load is applied because of this alignment; however, when a compressive stress is applied, the magnetic domains begin to move into a position that is perpendicular to the axis of the rod. A change in magnetization becomes apparent and this strange range is where the sensing characteristics are best. In order for a Galfenol alloy to be used as a sensor it must be pre-stressed to the appropriate level so that it is within the desired operating region. This critical pre-stress level varies with the bias magnetic field as will be discussed in more detail later.

For these experiments the interest was in capturing the characteristic shape of the sensing curves for Galfenol alloys over a wide range of stress and magnetic field levels under dynamic loading. As mentioned previously, the difficulty with dynamic loading comes in the application of the force. With many components of the system there was a small amount of compliance that effectively reduced the force generated because some of the energy was lost in deforming the different components. To combat this issue, the pre-stress mechanism shown in Figure 2.1 was used to apply an initial compressive load to the sample and the actuator was then used to apply a dynamic load from that point. By adjusting the initial bias stress the shape of the magnetization versus stress curve could be observed over a larger stress range.

CHAPTER 3

EXPERIMENT DESIGN

This chapter will focus on the design of the experiments and how the measurements were observed and recorded. When looking at any magnetostrictive material there are several important characteristics to measure. The coupling between the magnetic and mechanical regimes is the pripary area of interest. A secondary area of interest is the electrical system because this system is used to activate the overall experiment as well as record the measurements.

3.1 Experimental Objectives

The objective of this research is to characterize the relationship between the mechanical and the magnetic systems in a Galfenol alloy. There are two main ways in which the two systems interact: inverse and direct. The inverse effects characterize the actuation relationship whereas the direct effects are used in sensing. The following two subsections explain what is being measured in each of the two types of experiments. These sections are followed by a description of how these measurements were observed and recorded.

3.1.1 Actuation Measurements

Actuation of magnetostrictive materials makes use of the Joule effect. It is named for the founder of magnetostriction, James Joule, because this is the phenomenon that he observed and led to his discovery. In actuation, an applied magnetic field leads to a deformation of the magnetostrictive material in the direction of the field. This is due to the rotation of magnetic domains to align with the field.

With the magnetic transducer described in the previous chapter, a current is applied to the two excitation coils which creates a magnetic flux. This flux travels through the magnetic circuit and into the Galfenol sample, where it generates a field as the rod starts to deform. By increasing the current on the coils, the rod experiences more and more elongation, or magnetostriction, until saturation is reached. The value of elongation depends on the level of stress applied to the sample. A larger compressive pre-stress leads to a larger maximum magnetostriction. For the inverse effect in magnetostrictive materials, the important quantities to measure include: pre-stress, magnetic field, and magnetostriction (strain).

3.1.2 Sensing Measurements

Sensing using magnetostrictive materials makes use of the Villari effect. This direct effect states that there is a change in sample magnetization with an applied stress. In other words, as the stress in the sample is changed the

magnetization, which is a function of both magnetic field and magnetic flux density, changes accordingly.

The main focus of this thesis concentrates on the sensing characteristics of Galfenol alloys under dynamic loading. To achieve this goal, a sinusoidal load was applied through a piezoelectric actuator. After verifying the proper function of the overall experimental set-up at quasi-static frequencies, the frequency of the applied load was varied. For each test, a bias field in the sample was set by applying a constant current to the excitation coils of the magnetic transducer. This allowed for the sensing characteristics to be determined for different levels of initial bias field. After setting the bias field, the applied load began, and the magnetic field and flux density were measured. These two quantities allowed for the calculation of magnetization of the sample.

3.2 Electrical

For these experiments there were two main uses of an electrical system: creation of an initial bias field, and power supply to the piezoelectric actuator. Creating the initial bias field was completed by applying a constant current to the two excitation coils, and monitoring the magnetic field in the sample. The current was held constant through the duration of the experiment. Due to the changing permeability of Galfenol under an applied load, the field in the sample changes as the load is applied. As the permeability changes, the amount of the magnetomotive force dropped across the sample as part of the

magnetic circuit changes. With the application of compressive loads as is the case in the sensing experiments, the magnetic field increases with an increase in compressive stress.

The second use of an electrical system is in generating the power required to operate the piezoelectric actuator. The large frequency range and the linear response of piezeoelectric materials make them useful in dynamic operation. The actuator described in the previous chapter requires a +1000V input for full displacement. To obtain this kind of voltage, a high voltage KEPCO BOP 1000M Power Supply was used. The signal was generated in the SignalCalc Mobilyzer software and used as an input to the power supply. The power supply then amplified the signal so that the piezoelectric actuator received a high voltage sinusoidal input.

3.3 Mechanical

The mechanical system was composed of two components: force and strain. For sensing experiments, the strain was not a large concern. However, the strain must still be monitored to determine if the sample is experiencing purely axial loading. For this objective to be maintained, two OMEGA (SGD-3/350-LY11) axial strain gages were mounted to the sample. Using a National Instruments DAQ system and LabVIEW, the output of the strain gages were monitored to ensure no bending occurred both during installation as well as operation.

The second component of the mechanical system is force. This quantity

is directly related to the stress in the sample through the cross sectional area. To measure force, an OMEGA (LC703-1K) load cell was used in conjunction with a Vishay 2310 B signal conditioner. The load cell was installed in series with the Galfenol sample so that both experienced the same force. The output of the load cell was fed into the SignalCalc Mobilyzer software and recorded for later use in calculating the stress level.

3.4 Magnetic

As with the mechanical system, the magnetic system also had two quantities of interest: magnetic field and magnetic flux density. The magnetic field was measured with a HP145S transverse hall probe from Walker Scientific. The hall probe was positioned in the middle of the Galfenol sample, and was connected to a MG-4D Gaussmeter from Walker Scientific. The output of the Gaussmeter was also used as an input to the SignalCalc Mobilyzer where it was recorded.

The second quantity of interest was the magnetic flux density. The flux density was measured with a pick up coil of 74 turns with an inside diameter of 0.25 inches. The flux density in the sample produced a voltage in this pick-up coil that was collected by a MF-5D Fluxmeter from Walker Scientific. The MF-5D Fluxmeter is an integrating fluxmeter and thus the calibration coefficient had to be determined. Previous studies of this pick-up coil with a Galfenol sample showed that the calibration should be set to 23 cm^2. [17]

3.5 Signal Modulation

As mentioned in Chapter 1, signal modulation is achieved when two signals are multiplied together. The signal that is to be recovered after applying a demodulation scheme is called the signal wave while the other signal is called the carrier wave. The modulated signal is the product of the two signals. If the signal wave is,

$$A_{Signal} = X_s sin(2\pi f_s t), \tag{3.1}$$

and the carrier wave is,

$$A_{Carrier} = X_c sin(2\pi f_c t). \tag{3.2}$$

The product of the two waves is the modulated wave and is given by,

$$A_{Modulated} = \frac{X_c X_s}{2}[cos(2\pi(f_c - f_s)t) - cos(2\pi(f_s + f_c)t)]. \tag{3.3}$$

This process is shown graphically in Figure 3.1 For these images, the signal wave is 0.04 Hz and the carrier wave is taken as 5 Hz. The carrier wave must be much higher than the signal wave for signal wave to be recovered after applying the demodulation technique described after Figure 3.2.

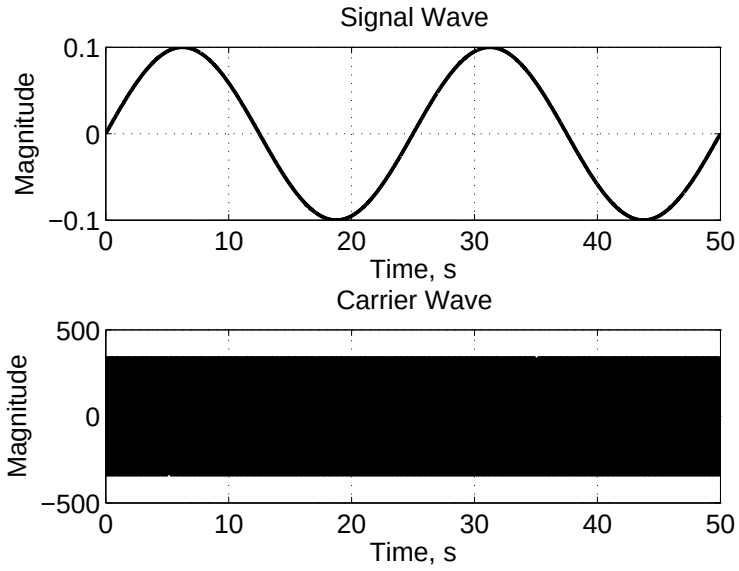

Figure 3.1: Sample Signal and Carrier Wave

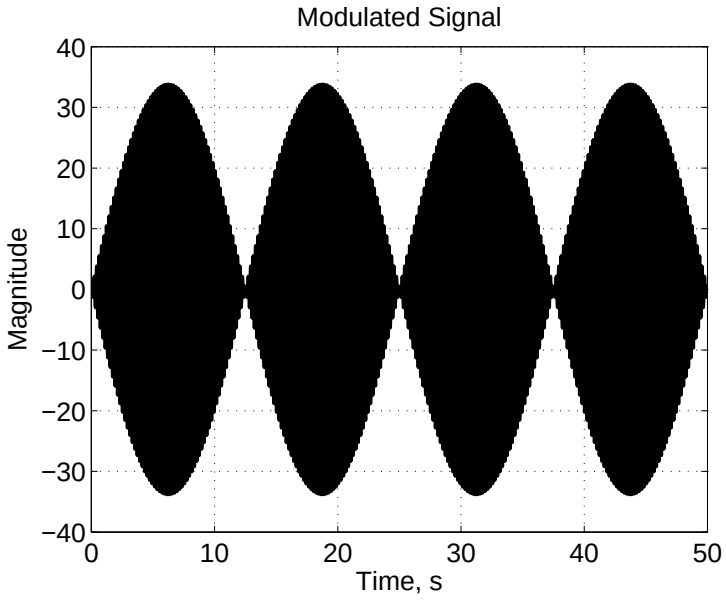

Figure 3.2: Modulated Signal

The modulated signal contains two frequencies that are on either side of the carrier wave frequency. There are several ways to demodulate a modulated signal to recover the original signal. This research utilizes the product detector. For this demodulation scheme, the modulated signal is multiplied by the carrier wave. For this example Equation 3.3 is multiplied by Equation 3.2 to produce,

$$A_{Demodulated} = \frac{X_c X_s}{4|X_c|^2}[2sin(2\pi f_s t) + sin(2\pi(2f_c - f_s)t) - sin(2\pi(2f_c + f_s)t)]. \tag{3.4}$$

It can be seen that the demodulated signal contains three frequencies, with one being the frequency of the original signal wave. Using a low pass filter, the higher frequencies can be filtered out and the original signal recovered. Figure 3.3 shows the demodulated signal before filtering, and Figure 3.4 shows the filtered signal. The filtered signal has a phase lag created by the low pass filter. This phase lag is accounted for when plotting the results.

The process described above was used in this research with the signal wave being the change in flux density due to the applied stress and the carrier wave being the change in flux density due to the sinusoidal magnetic field. Both the modulated signal and the carrier wave were recorded with the data acquisition software and the demodulation performed in MatLab. The results of this analysis are discussed in the following section of this thesis.

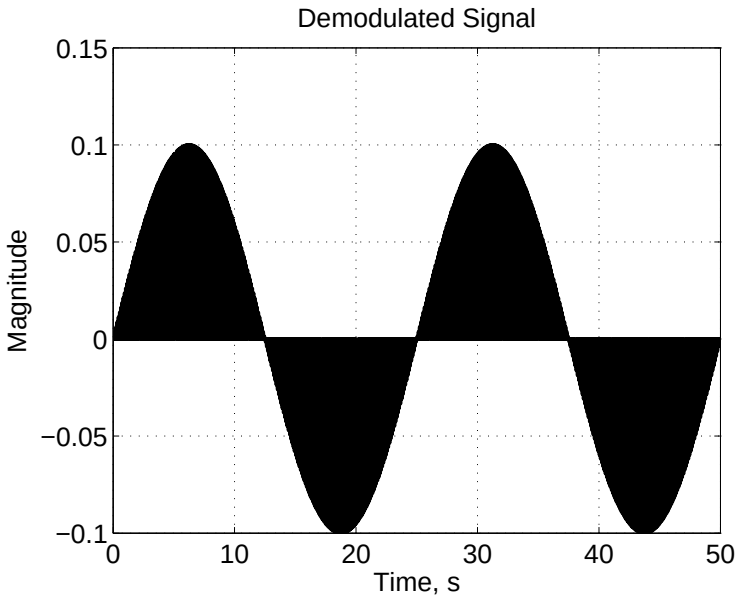

Figure 3.3: Demodulated Signal

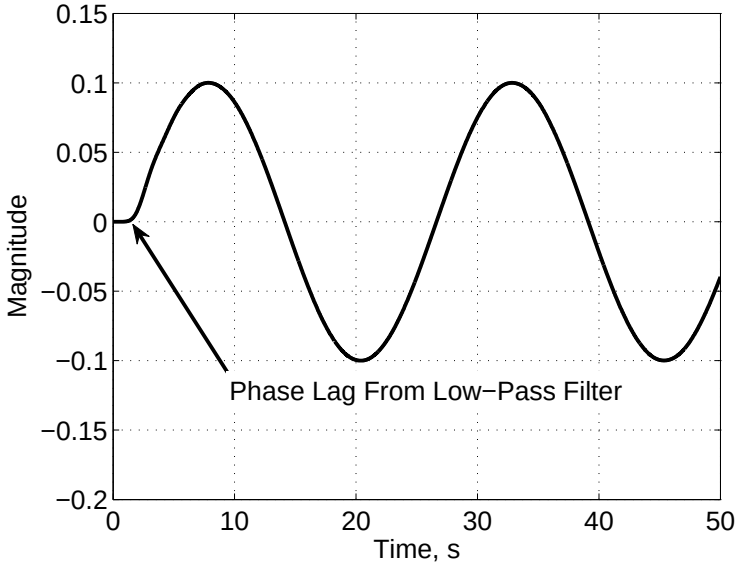

Figure 3.4: Demodulated Signal (Filtered)

CHAPTER 4

RESULTS AND DISSCUSSION

4.1 Quasi-Static Validation

The test described in the previous section was set up and conducted under quasi-static loading of the sample. For these tests, the magnetic bias level was set at zero stress, and then the pre-stress level adjusted to the region of largest change as observed in the quasi-static results. The piezo actuator was then activated to produce a sinusoidal stress with a peak-to-peak stress level of approximately 10 MPa. The level of stress excitation varied slightly from test to test because of small variations in the set up due to human input. Figure 4.1 shows results for two different levels of field. The results of the dynamic testing apparatus match well with the previous results from the quasi-static tests. After conducting these tests to validate the testing apparatus, the testing moved to characterizing the Galfenol sample at different frequency levels. This characterization is discussed in the following subsection of this thesis. For all of the test conducted as a part of this thesis, the $Fe_{81.6}Ga_{18.4}$ Galfenol alloy was used.

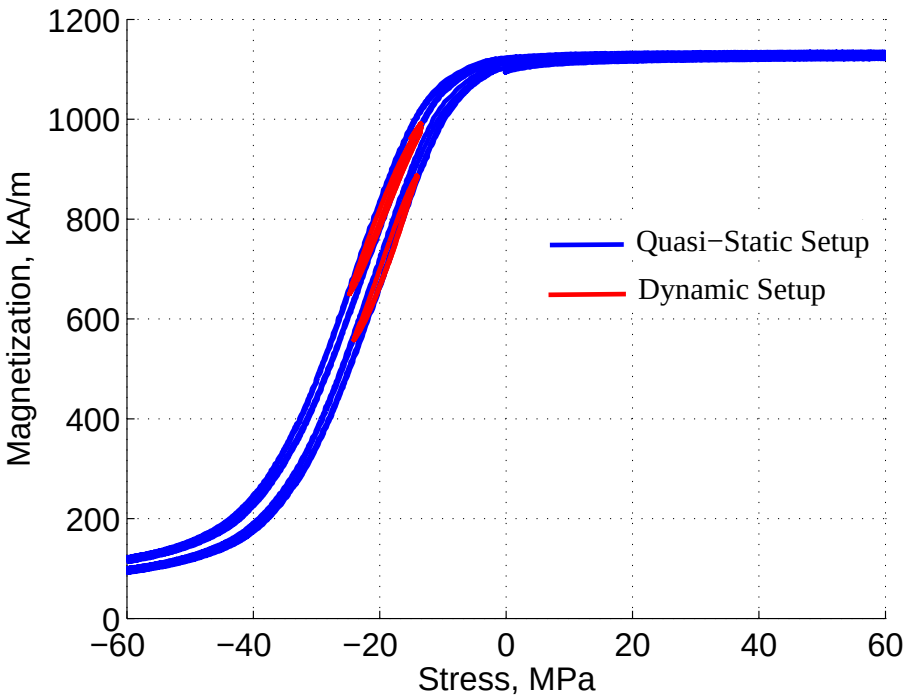

Figure 4.1: Testing Apparatus Validation with Quasi-Static Results

4.2 Dynamic Characterization

The dynamic characterization of Galfenol alloys looks at how the change in magnetization varies at various frequencies. From the dynamic actuation testing, the hysteresis loss is expected to increase as the frequency increases. To characterize the Galfenol sample in the dynamic regime, the bias field was first set with the sample under zero stress. This was accomplished by adjusting the current input to the coils until the desired field level was achieved. The current was then kept constant as the test progressed. Next, the sample was adjusted to the appropriate bias stress level using the pre-stress device.

The level of pre-stress was found from the quasi-static sensing curves. The pre-stress was adjusted to the point on the sensing curves where there was the largest change in magnetization for each increment of stress. Figure 4.1 illustrates two of the field levels shown for comparison with the quasi-static data. From this data it can be seen that the stress level must start from $\sim$ -18 MPa and increase in compressive stress to be simulated along the most sensitive part of the curve for that particular field level. The required bias compressive stress increases with an increase in the magnetic field. The two cases shown above correspond to $\sim$3.58 kA/m and $\sim$4.22 kA/m respectively. These field levels are the zero stress field levels. As the compressive stress in the sample increases, the field level increases as well. Figure 4.2 and Figure 4.3 show how the magnetization changes with a change in frequency. The two main areas of interest from this data are: sensitivity (slope) and hysteresis loss. These two topics are discussed in more detail below.

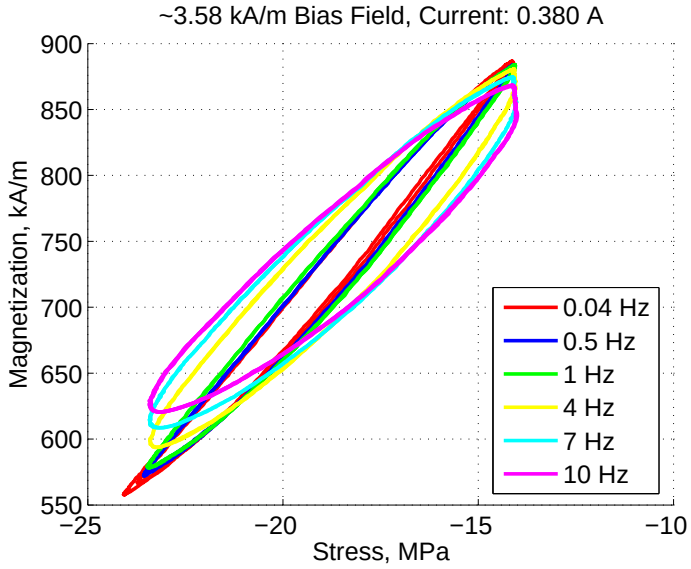

Figure 4.2: Magnetization vs. Stress at different frequencies for a bias field of ∼3.58 kA/m

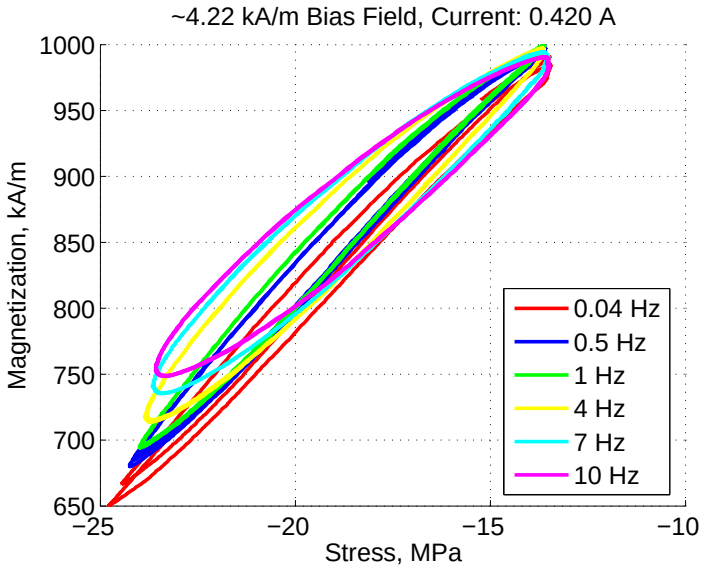

Figure 4.3: Magnetization vs. Stress at different frequencies for a bias field of ∼4.22 kA/m

4.2.1 Sensitivity

The issue of sensitivity is important because this value is the basis for a force sensor. Given a sensor, the sensitivity relates the output from the sensor to the given input. For the case of a magnetostrictive material, the sensitivity relates the output magnetization to the input stress. The sensitivity was approximated with a linear fit of the data. A representation of this process can be seen in Figure 4.4 for the case with a bias magnetic field of $\sim$3.58 kA/m and a stress excitation of 1 Hz. Figure 4.5 shows a linear approximation for the magnetization versus stress curves when the bias field was set at $\sim$3.58 kA/m. This linear approximation provides a representation of the sensitivity that can be compared at various frequencies. The slope of the linear approximation is not the exact sensitivity of the actual magnetization versus stress curves due to the hysteresis loss observed in the data, but it still provides a good indication of how the slope is changing.

It can be seen from Figure 4.5 and Table 4.1 that the sensitivity of the Galfenol sample decreases with increasing frequency. The following table summarizes the change in sensitivity for several different bias field levels. At each level of bias stress, the same trend of decreasing sensitivity is observed. This consistency will be useful in the design of a force sensor.

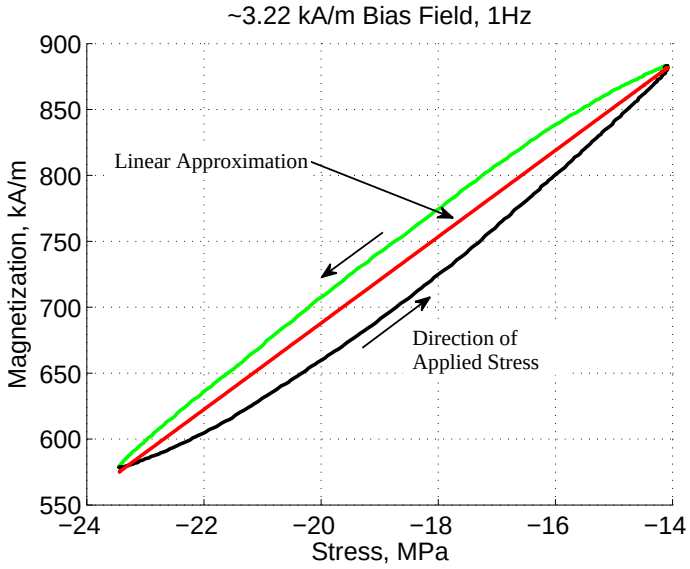

Figure 4.4: Linear Representation of magnetization vs. stress ∼3.58 kA/m bias field, 1 Hz Excitation

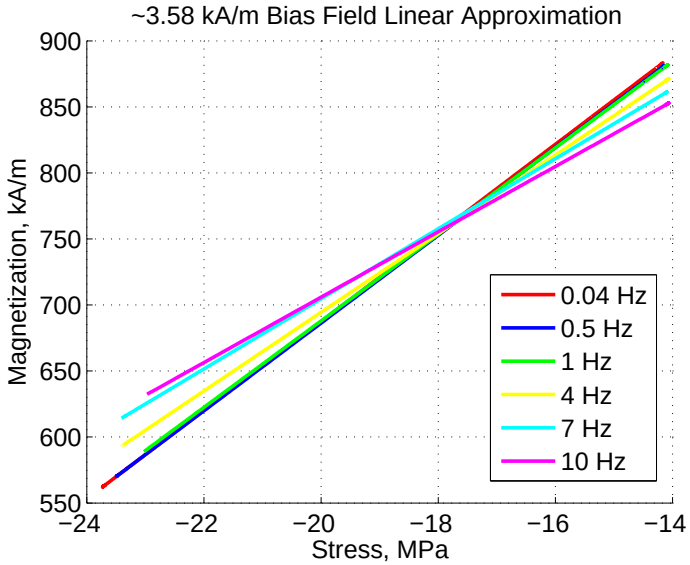

Figure 4.5: Linear approximation of magnetization vs. stress to visualize change in sensitivity for ∼3.58 kA/m bias field

Table 4.1: Sensitivity of Galfenol Sample at different Bias Field Levels

Bias Field	Sensitivity [(kA/m)/MPa]					
Level [kA/m]	0.04 Hz	0.5 Hz	1 Hz	4 Hz	7 Hz	10 Hz
1.72	22.72	22.36	22.14	19.80	17.53	16.19
2.78	29.01	28.66	28.03	15.61	13.55	21.85
3.58	33.57	33.24	32.75	29.78	26.53	24.75
4.22	30.09	29.90	29.50	27.18	24.51	23.09
5.01	25.19	25.11	24.82	23.22	21.81	19.97
5.73	30.73	30.49	30.30	28.27	25.54	24.01
6.60	22.66	21.89	21.53	20.52	19.12	18.33
7.32	22.34	21.82	21.53	20.36	19.50	18.26

4.2.2 Hysteresis Loss

Hysteresis loss is another important area when designing a sensor. Hysteresis is observed as the difference in output when the input is increasing as compared to when the input is decreasing. This creates an elliptical shape in the sensing curve. In the case of a magnetostrictive sensor, the ellipse is observed in the magnetization versus stress curves. The path of changing magnetization is different when the compressive stress level is increasing as compared to when the stress level is becoming less compressive. The hysteresis loss is found by looking at the area inside the ellipse. This area represents energy loss due to the effect of hysteresis. Figure 4.6 shows a depiction of this phenomenon and how the magnetization level changes with the different means of loading the Galfenol sample.

As can be seen in Figure 4.6 the magnetization level when the input stress is becoming more compressive is higher than the magnetization when the

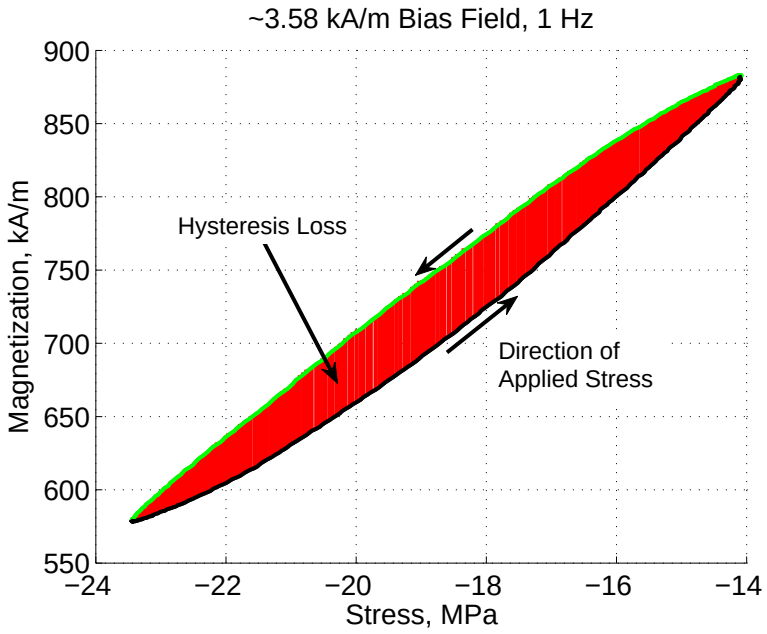

Figure 4.6: Depiction of hysteresis loss for ∼3.58 kA/m bias field at 1 Hz stress excitation

compressive stress is decreasing. This creates the ellipse seen in the graph. The area inside the ellipse was compared for each of the different frequencies at the various field levels tested and is summarized below in Table 4.2. This table shows that the hysteresis loss increases with the increase in frequency of the input stress. This will be another useful tool in developing a force sensor.

Table 4.2 shows how the hysteresis loss increases with an increase in the input frequency. From one bias field to the next the hysteresis loss changes because of the variation in the stress range. The following section on signal modulation describes an alternate way of looking at the sensing characteristics of the Galfenol sample.

Table 4.2: Hysteresis Loss of Galfenol Sample at different Bias Field Levels

Bias Field	Hysteresis Loss [(kA/m)*MPa]					
Level [kA/m]	0.04 Hz	0.5 Hz	1 Hz	4 Hz	7 Hz	10 Hz
1.72	117.22	152.54	227.19	362.75	392.70	403.41
2.78	114.04	140.32	167.06	344.57	337.69	393.97
3.58	259.36	285.18	339.70	555.87	639.06	662.39
4.22	228.10	234.23	292.95	498.41	574.76	577.76
5.01	79.99	101.65	140.74	208.66	253.21	266.20
5.73	112.93	180.63	203.50	363.67	382.19	390.89
6.60	73.22	111.60	113.71	185.21	212.55	217.44
7.32	23.46	84.32	86.82	130.39	159.37	173.34

4.3 Signal Modulation

An alternate means of relating the input stress to the output change in magnetization makes use of the signal modulation scheme described in the previous chapter. The advantage of this method is that the bias sensor can operate around the zero bias field level. Under constant field operation, there is very little change in the magnetization level with a change in the input stress. This requires additional energy to be input to the system to increase the bias field level to get a usable reading. The signal modulation process uses the combined signal of two excitations to enhance the signal. Moreover, this process helps to reduce noise in the signal as the two input signals are multiplied together. Evans and Dapino [11] have modeled the stress dependent susceptibility of Galfenol in the magnetic domain rotation region. This relationship makes use of a modulated signal across the pick-up coil, and allows for an analytical method for relating the input stress to an

output signal. They have found that the susceptibiltiy is given by,

$$\chi(T) = \frac{\mu_0 M_s^2}{2K_4 - 3\lambda_{100} T}. \tag{4.1}$$

where $\chi(\mathbf{T})$ is the stres-dependent susceptibility, μ_0 is the permeability of free space, $\mathbf{M}_s$ is the saturation magnetization, $\mathbf{K}_4$ is the anisotropy constant, λ_{100} is the saturation magnetostriction, and $\mathbf{T}$ is the stress. Using this relationship and a high frequency signal to the excitation coils in relation to the frequency of stress input, the voltage in the pick-up coil ($\mathbf{V}_d$) is given by 4.2. This voltage is an amplitude modulated signal of $\mathbf{H}_e$, excitation field, and $\chi(\mathbf{T})$, stress-dependent susceptibility. In the following equation, $\mathbf{N}$ is the number of turns in the pick-up coil, $\mathbf{A}$ is the cross sectional area of the Galfenol sample, and ω_e is the excitation frequency to the excitation coils.

$$V_d = \mu_0 N A \omega_e \chi(T) H_e \tag{4.2}$$

For the experiments conducted as a part of this research, the excitation coils of the magnetic flux circuit were excited with a high frequency current to act as the carrier wave, while the signal wave was produced through the piezoelectric actuator. Both the field and the flux density were modulated and subsequently put through a demodulation process offline in MatLab. This modulation scheme was completed in the quasi-static regime and the results are shown below. [15]. Figure 4.7 shows the modulated signal that was obtained from the test. Figures 4.8 and 4.9 shows the demodulated

magnetization and susceptibility as a funtion of the applied stress.

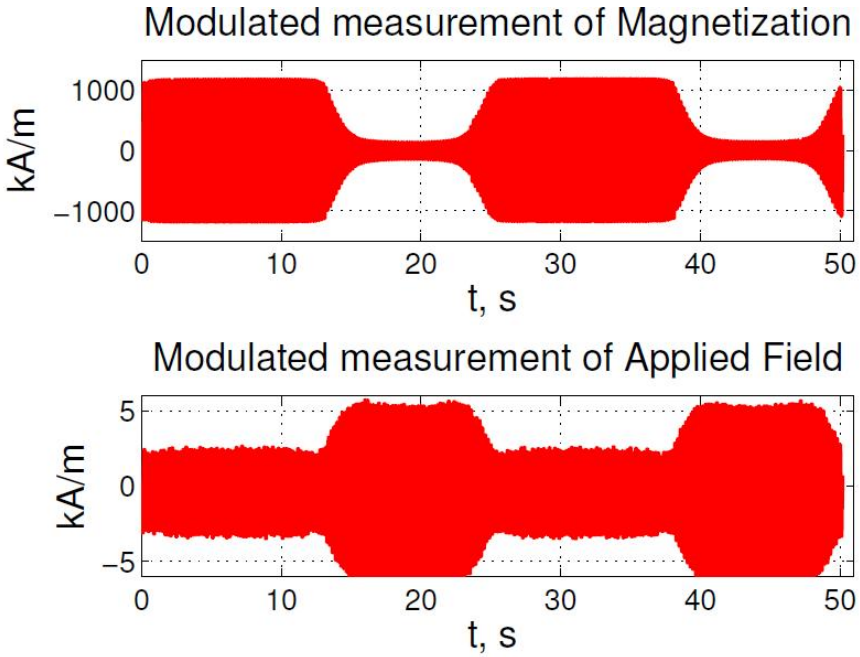

Figure 4.7: Modulated signals for magnetization and magnetic field for $Fe_{81.6}Ga_{18.4}$ with stress excitation at 0.04 Hz [15]

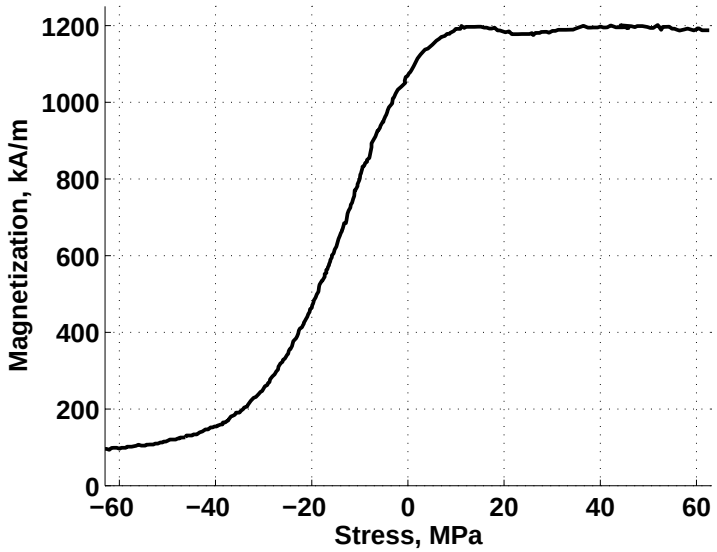

Figure 4.8: Demodulated magnetization for $Fe_{81.6}Ga_{18.4}$ sample [15]

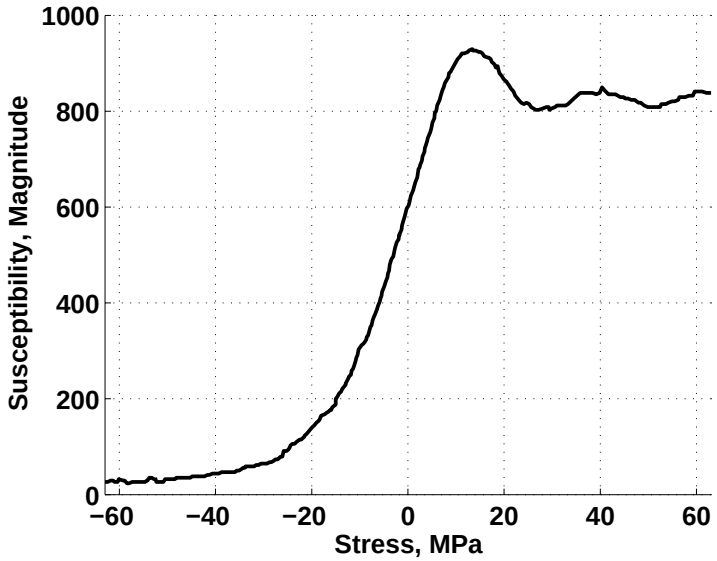

Figure 4.9: Demodulated susceptibility for $Fe_{81.6}Ga_{18.4}$ sample [15]

For the dynamic regime testing, three different frequency levels of stress excitation were tested: 0.04 Hz, 0.50 Hz, and 1.00 Hz. The current to the coils was set with an amplitude of approximately 350 mA and a frequency of 5 Hz, 50 Hz, and 100 Hz respectively. The challenge with these tests is capturing two full cycles of the input signal while maintaining a sufficient number of points to capture the carrier signal as well. The large difference in frequencies requires care to be taken in setting the data aquisition software. Figure 4.10 shows the modulated measurements for a stress excitation of 0.04 Hz and a carrier wave of 5 Hz. The modulated signal was then demodulated using the scheme outlined in the previous chapter. The demodulated signal before filtering out the higher frequencies can be seen in Figure 4.11.

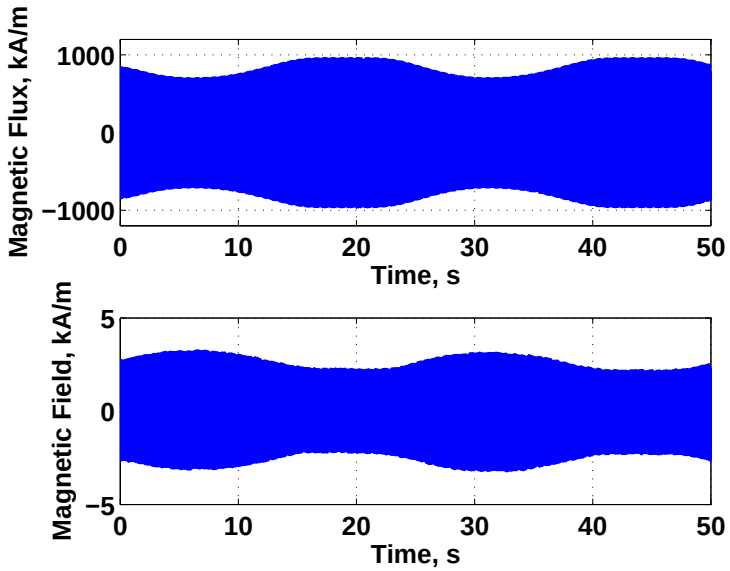

Figure 4.10: Modulated signal for $Fe_{81.6}Ga_{18.4}$ sample with 0.04 Hz excitation

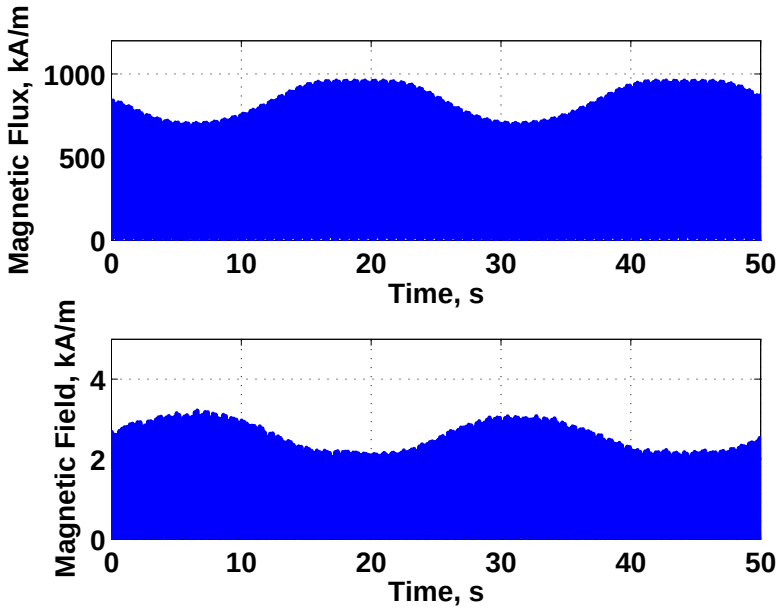

Figure 4.11: Demodulated signal for $Fe_{81.6}Ga_{18.4}$ sample with 0.04 Hz excitation

As mentioned in Chapter 3, there is a phase lag associated with the low pass filtering of the demodulated signal. This phase lag has been accounted for in the results shown below. Figure 4.12 shows the demodulated magnetization at each of the differnet input frequencies. These results show a similar trend with the dynamic characterization data in that the sensitivity, slope, of the Galfenol sample decreases with an increase in the input frequency. Figure 4.13 shows a similar trend for the susceptibility.

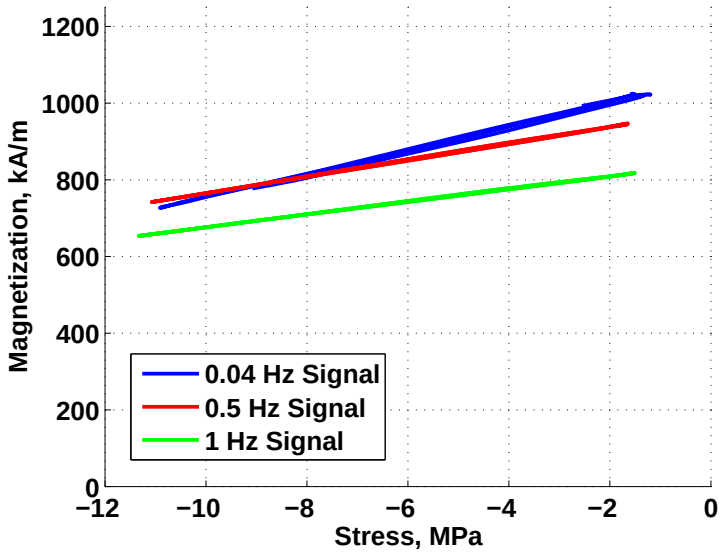

Figure 4.12: Demodulated Magnetization for $Fe_{81.6}Ga_{18.4}$ sample at various input frequencies

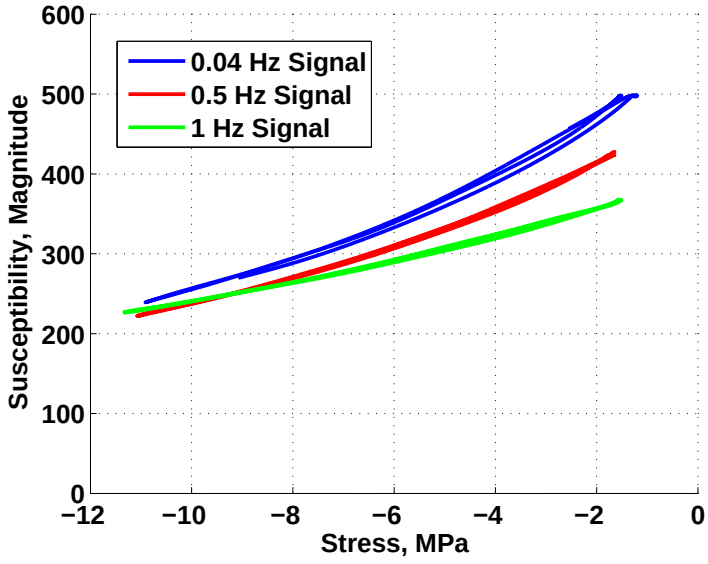

Figure 4.13: Demodulated susceptibility for $Fe_{81.6}Ga_{18.4}$ sample at various input frequencies

CHAPTER 5

SUMMARY AND CONCLUSION

This thesis looked at the dynamic characterization of Galfenol alloys with special interest in the sensing characteristics. For the data collected and reported in the preceding pages of this thesis, a dynamically excited stress was applied to a $Fe_{81.6}Ga_{18.4}$ sample of <100> orientated polycrystalline Galfenol. The corresponding magnetization was observed to characterize this material for use in the design of a force sensor. Before these measurements could be taken, an appropriate testing apparatus was designed to apply the loading and allow for the different sensors described in the thesis to be implemented. This testing apparatus reduced the overall compliance in the system to facilitate the use of a piezoelectric actuator as the means of applying the dynamic stress. The design of this apparatus was discussed in Chapter 2 while the means of measurement was shown in Chapter 3.

The second phase of this research looked at the general dynamic characterization of the material for sensing applications. From the data, it was observed that both the hysteresis losses and the sensitivity were affected with the changing frequency. The hysteresis loss increased with an increase in the

frequency of the applied field while the opposite was true of the sensitivity. These two characteristics will be important as guidelines are developed for creating a force sensor using Galfenol alloys.

The third area of interest observed in this thesis was an alternate means of collecting the signal created by the sensor. This is achieved through the modulation/demodulation scheme described above. This process is currently used in radio signals. The modulation process uses a time varying field in the sample rather than a constant field. The purpose of this method was two-fold: to reduce the noise in the observed data and allow for the field to be at lower levels. With this method, the field can be oscillated around zero field and can have a relatively small amplitude. This is important because in the original approach, a higher bias field was required to see an observable change in the magnetization. The results for both the general characterization and the modulation scheme were shown in Chapter 4.

The work done in this research has provided some insight into the dynamic behavior of Galfenol alloys; however, further work needs to be done to begin the development of force sensors using Galfenol. A set of experiments designed to determine the frequency bandwidth of a sensor using Galfenol will be instrumental in creating guidelines for future work with Galfenol. Moreover, these experiments will help to characterize the performance of a Galfenol based sensor at higher frequencies. Determining the durability and fatigue of such a sensor will also be a fundamental area of research as the study of Galfenol progresses. In conclusion, this research was a significant

step forward in the understanding of Galfenol alloys and how they might be used in future applications. There are still unknowns associated with these alloys that require further research.

BIBLIOGRAPHY

[1] J. Atulasimha. *Characterization and Modeling of the Magnetomechanical Behavior of Iron-Gallium Alloys*. PhD thesis, University of Maryland, College Park, MD, 2006.

[2] B. Bhattacharya. Terfenol and galfenol: Smart magnetostrictive metals for intelligent transduction. Technical report, Indian Institute of Technology Kanpur, Kanpur, India, 2005.

[3] F. Calkins, A. Flatau, and M. J. Dapino. Overview of magnetostrictive sensor technology. *Journal of Intelligent Material Systems and Structures*, 2007.

[4] M. J. Dapino. On magnetostrictive materials and their use in adaptive structures. *Structural Engineering and Mechanics*, pages 303–329, 2004.

[5] M. J. Dapino, F. Calkins, and A. Faltau. Magnetostrictive devices. In John G. Webster, editor, *Wiley Encyclopedia of Electrical and Electronics Engineering*, pages 278–305. John Wiley & Sons, Inc., New York, NY, 1999.

[6] M. J. Dapino, R. Smith, F. Calkins, and A. Flatau. A magnetoelastic model for villari-effect magnetostrictive sensors. Technical report, Center for Research in Scientific Computation, Raleigh, NC, 2002.

[7] S. Datta, M. Huang, J. Raim, T. Logasso, and A. Flatau. Effect of thermal history and gallium content on magneto-mechanical properties of iron-gallium alloys. *Materials Science and Engineering*, 2006.

[8] P. G. Evans. *Nonlinear Magneto-Mechanical Modeling and Characterization of Galfenol and System-Level Modeling of Galfenol-Based Transducers*. PhD thesis, The Ohio State University, Columbus, OH, 2009.

[9] P. G. Evans and M. J. Dapino. State-space constitutive model for magnetization and magnetostiction. *IEE Transactions of Magnetics*, 2008.

[10] P. G. Evans and M. J. Dapino. Measurement and modeling of magnetomechanical coupling in magnetostrictive iron-gallium alloys. *SPIE Smart Materials and Structures Symposium*, 2009.

[11] P. G. Evans and M. J. Dapino. Stress dependent susceptibility of galfenol to force sensing. *Journal of Applied Physcis*, 2010.

[12] F. V. Hunt. *Electroacoustics: The Analysis of Transduction, and Its Historical Background*. American Institute of Physics for the Acoustical Society of America, 1982.

[13] R. Kellogg, A. Flatau, A. Clark, M. Won-Fogle, and T. Lograsso. Quasistatic transduction characterization of galfenol. *2003 ASME International Mechanical Engineering Congress*, 2003.

[14] A.E. Kinnelly and H. Nukiyama. Electromagnetic theory of the telephone receiver: With special reference to motional impedance. In *Proceedings of the American Institute of Electrical Engineers*, 1919.

[15] A. Mahadevan. Force and torque sensing with galfenol alloys. Master's thesis, The Ohio State University, Columbus, OH, 2009.

[16] A. Mahadevan, P. G. Evans, and M. J. Dapino. Stress dependence of magnetic susceptibility on stress in fega. *Applied Physics Letters*, 2010.

[17] C. Poeppelman. Characterization of magnetostrictive iron-gallium alloys under dynamic conditions. Undergraduate Honors Thesis at The Ohio State University, 2010.

APPENDIX A

TIME DOMAIN PLOTS OF DYNAMIC CHARACTERIZATION

The following figures are the time domain plots of the data collected during the general dynamic characterization with a bias field of $\sim$3.58 kA/m. The data for the other bias fields tested as a part of this thesis look similar, and for this reason only one case is shown below for simplicity. The excitation stress and the corresponding magnetization are shown. Each plot represents a different frequency of stress exciation. The results of these plots as they relate to the sensing characteristics can be found in Chapter 4.

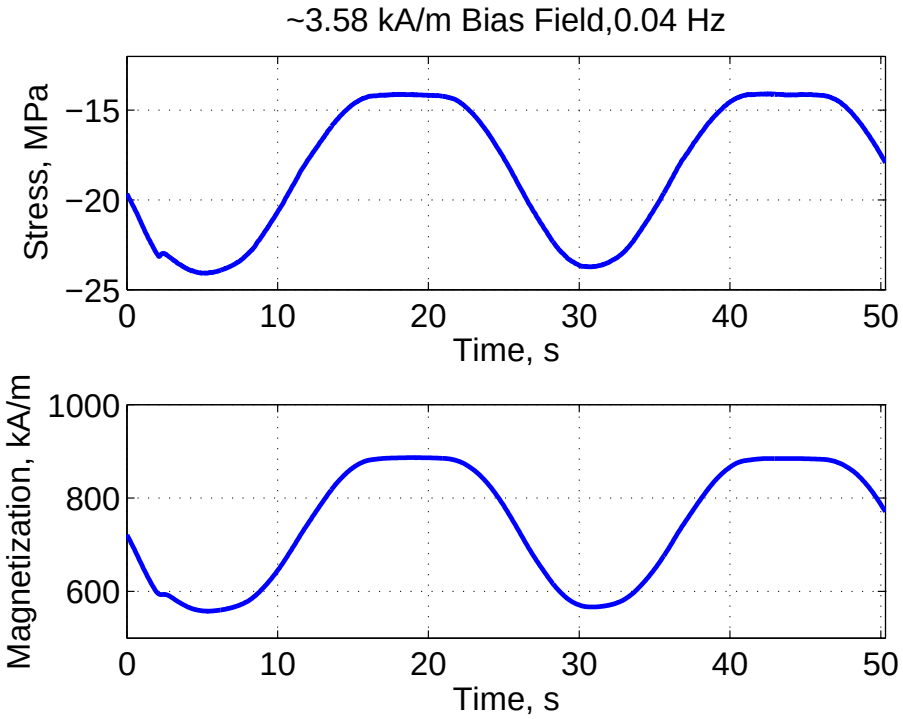

Figure A.1: Dynamic Characterization, 0.04 Hz Stress Excitation

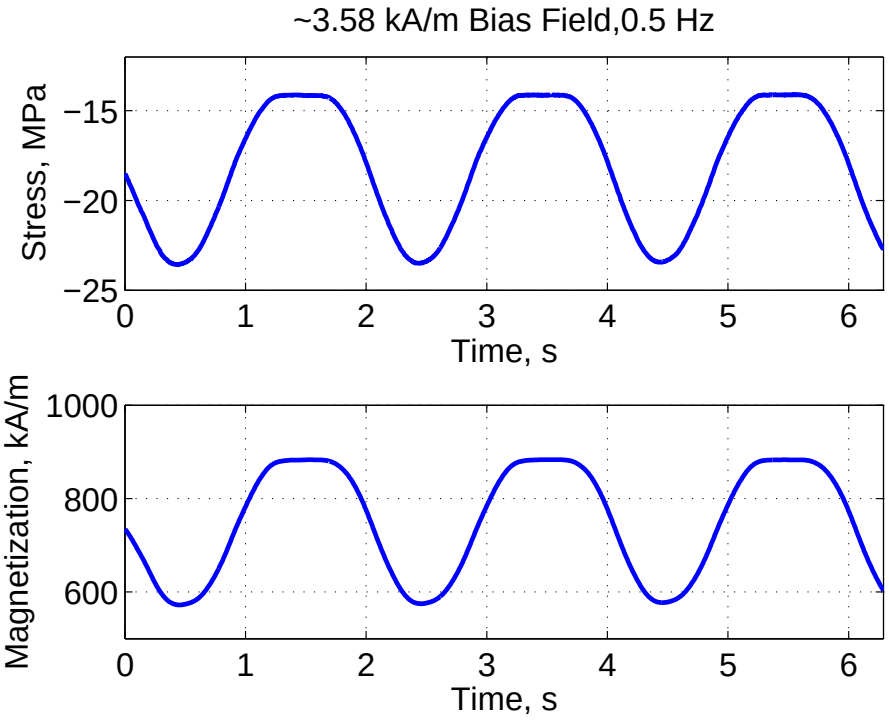

Figure A.2: Dynamic Characterization, 0.5 Hz Stress Excitation

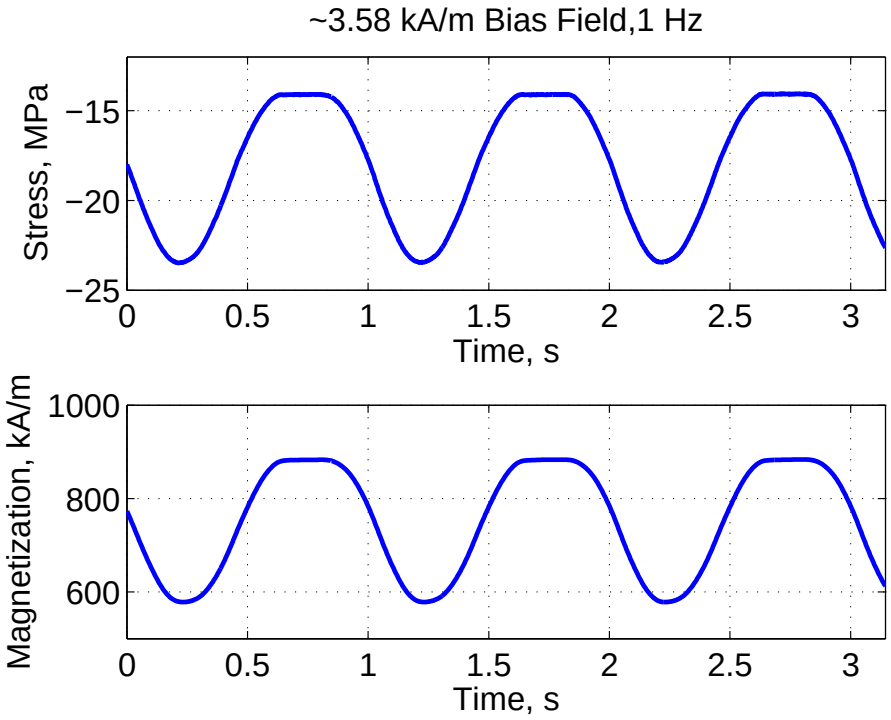

Figure A.3: Dynamic Characterization, 1 Hz Stress Excitation

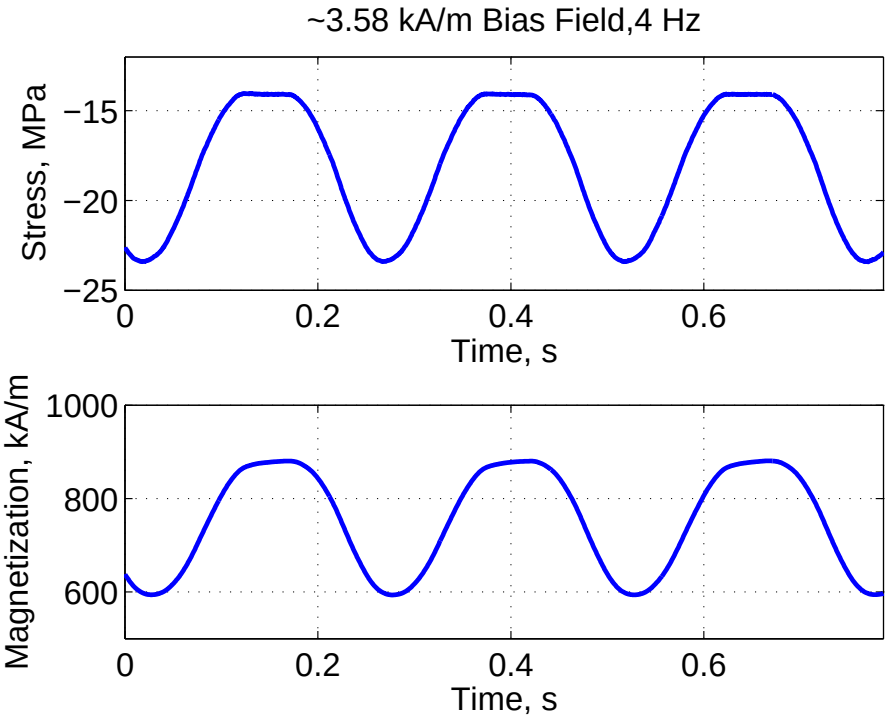

Figure A.4: Dynamic Characterization, 4 Hz Stress Excitation

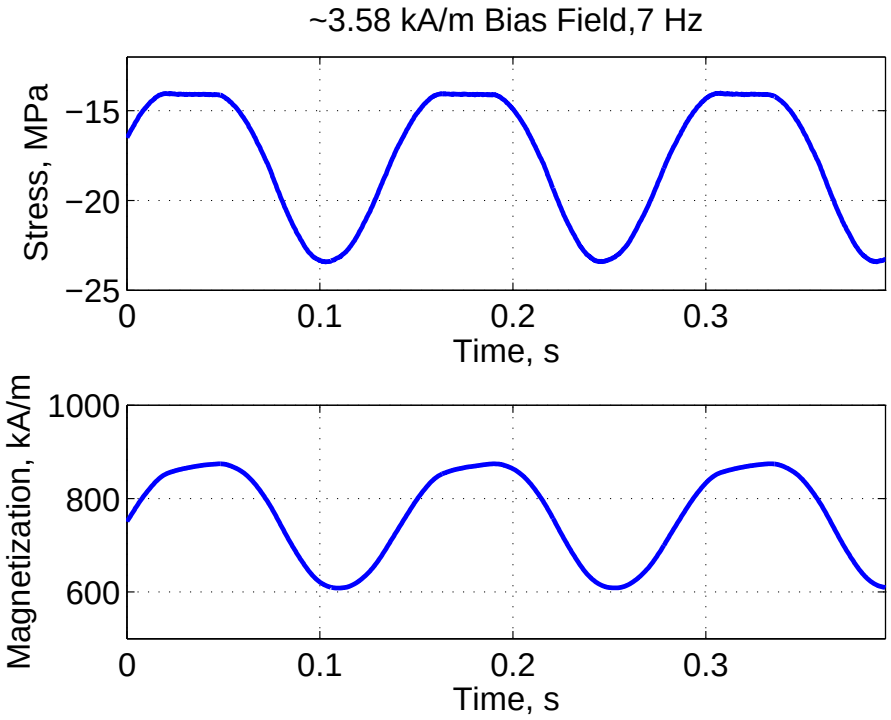

Figure A.5: Dynamic Characterization, 7 Hz Stress Excitation

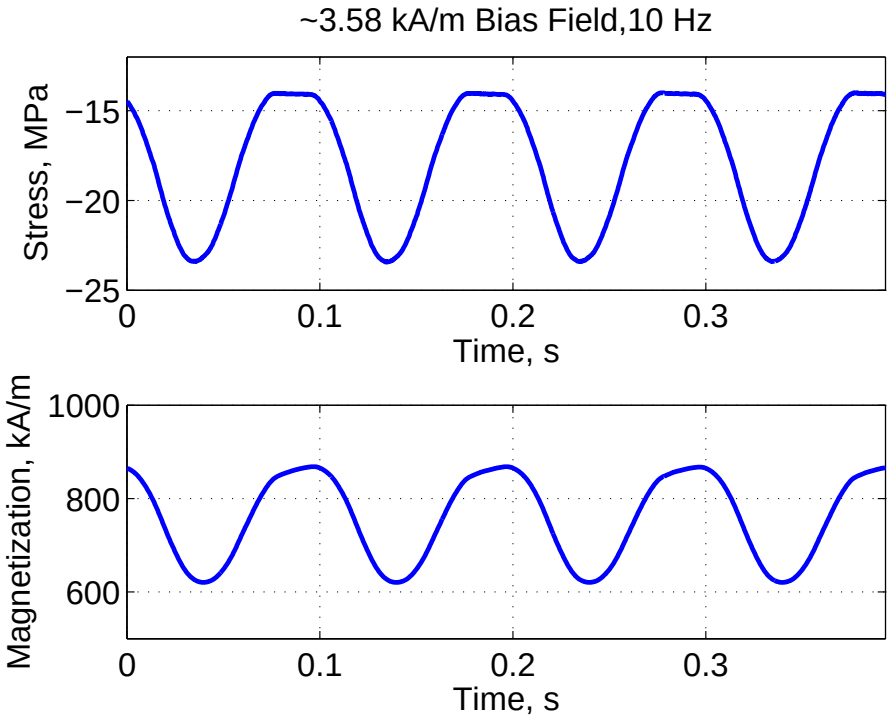

Figure A.6: Dynamic Characterization, 10 Hz Stress Excitation

APPENDIX B

TIME DOMAIN PLOTS OF MODULATION SCHEME

The following plots show the three different cases studied using the modulation scheme. The results of this data and how it can be used is discussed in Chapter 4. As mentioned, the three cases coincide with stress excitations of 0.04 Hz, 0.5 Hz, and 1 Hz. The corresponding carrier wave was 5 Hz, 50 Hz, and 100 Hz respectively.

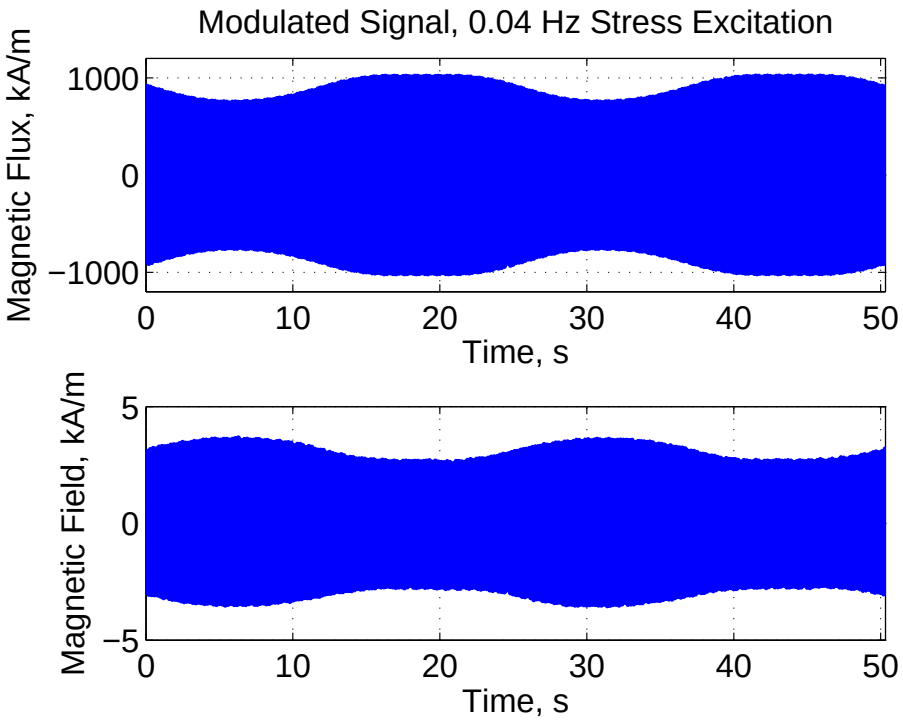

Figure B.1: Modulated Signal for 0.04 Hz Stress Excitation

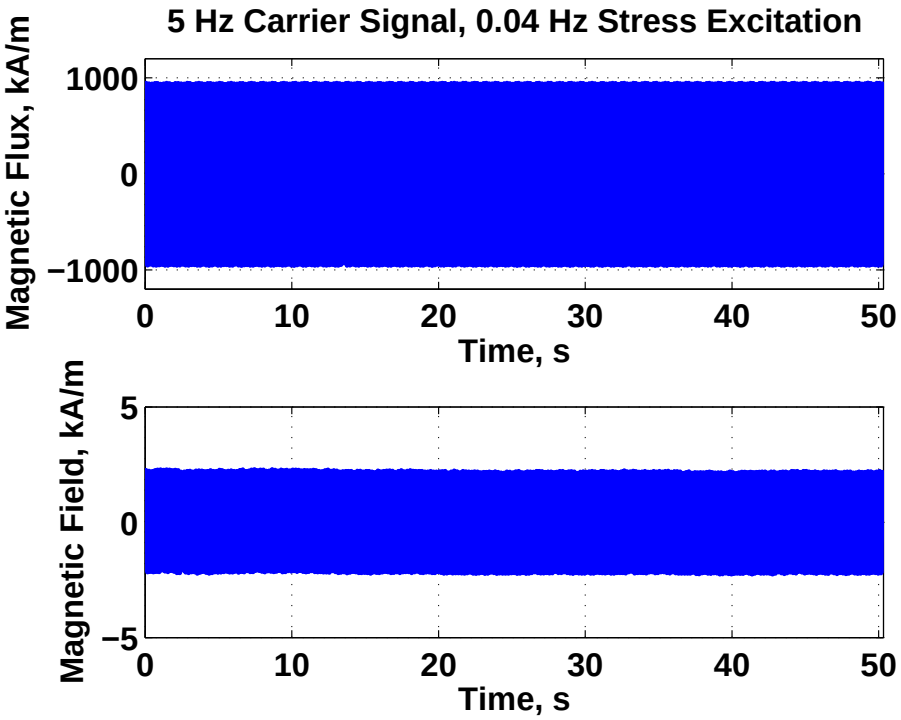

Figure B.2: 5 Hz Carrier Signal for 0.04 Hz Stress Excitation

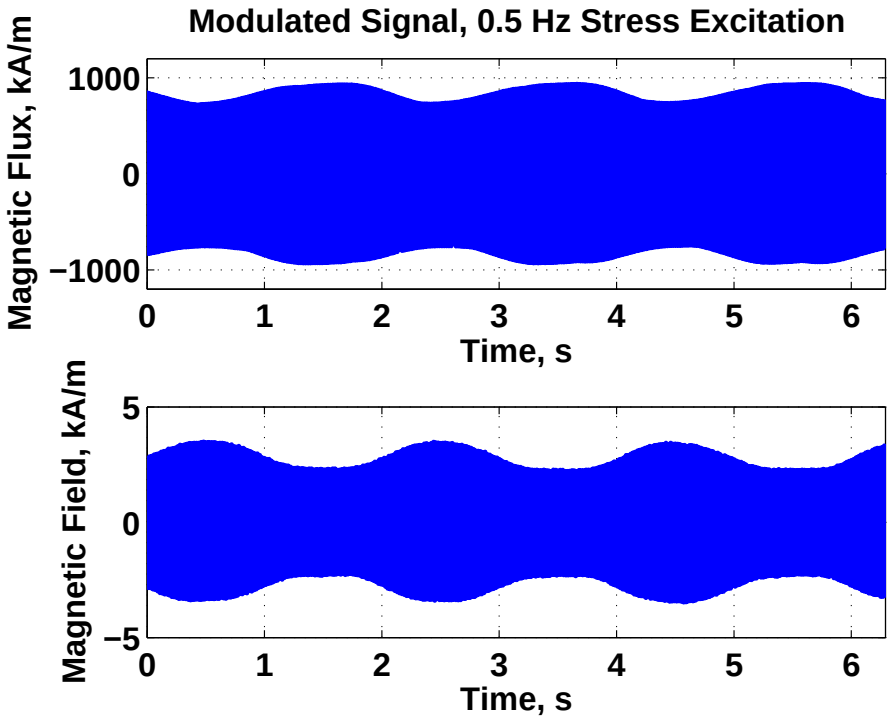

Figure B.3: Modulated Signal for 0.5 Hz Stress Excitation

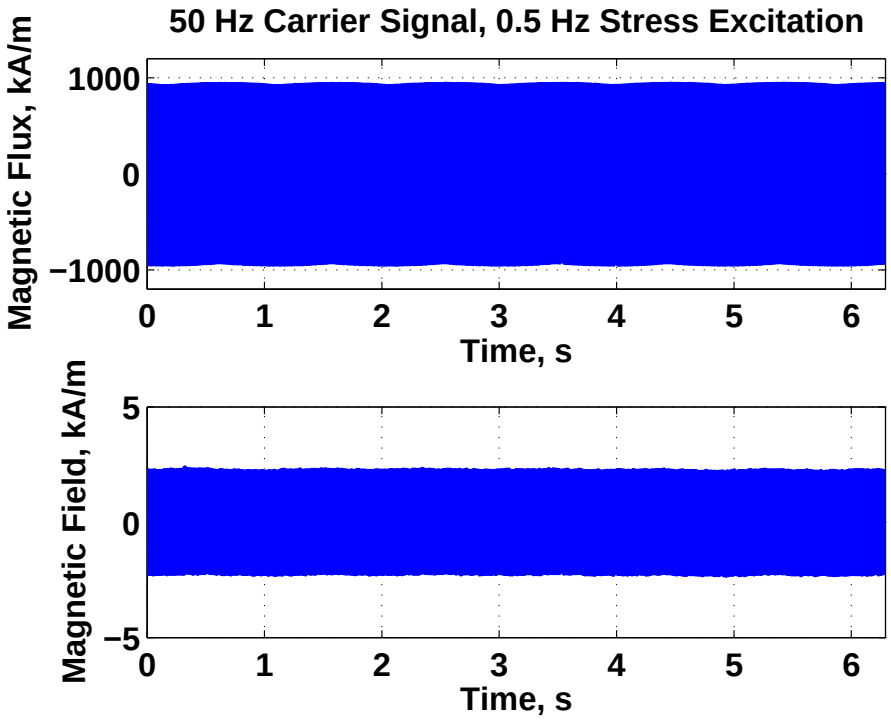

Figure B.4: 50 Hz Carrier Signal for 0.5 Hz Stress Excitation

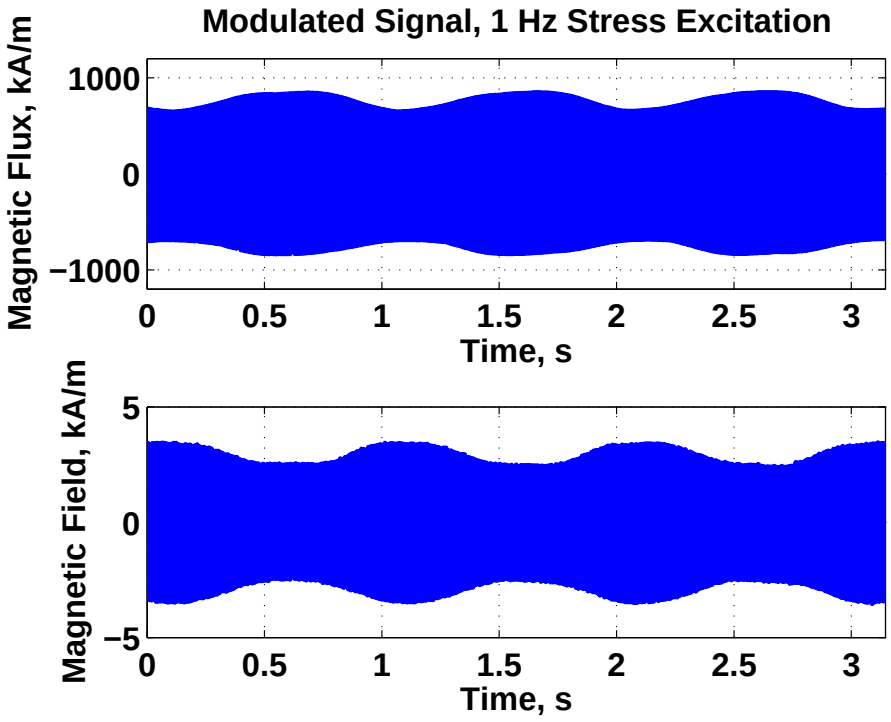

Figure B.5: Modulated Signal for 1 Hz Stress Excitation

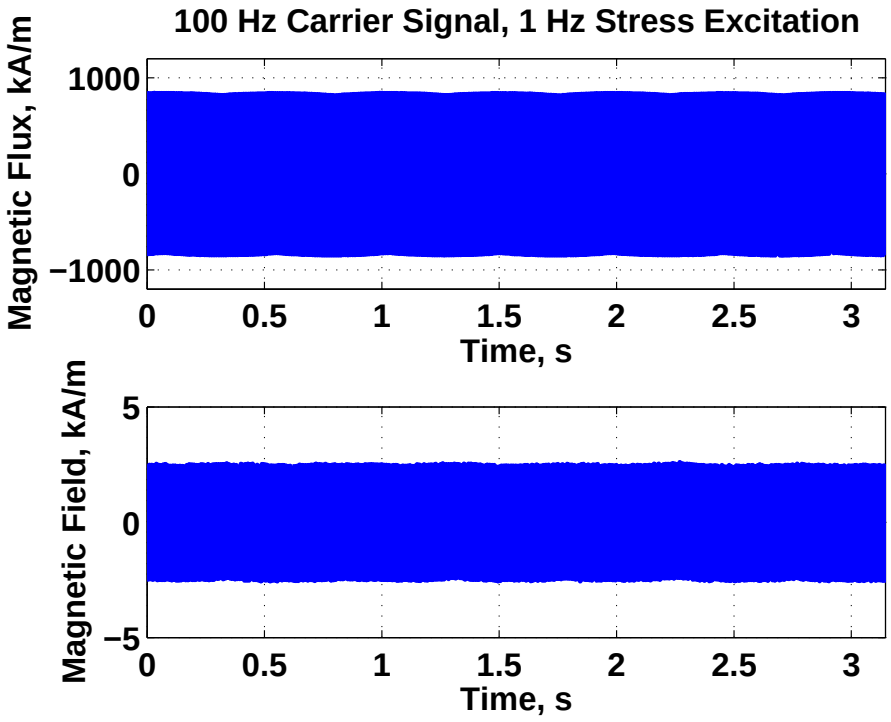

Figure B.6: 100 Hz Carrier Signal for 1 Hz Stress Excitation

APPENDIX C

IMPEDANCE ANALYSIS OF SENSING TRANSDUCER

C.1 Introduction

The impedance of an electromechanical transducer using a magnetostrictive element relates the input current to the output voltage. The current is used to create the magnetic flux in the circuit, and the changing magnetic flux creates a voltage in the pick-up coil. To characterize the performance of the transducer in terms of frequency bandwidth, the frequency response of the impedance can be measured and the resulting data analyzed. Using the impednace in this manner comes from the study of electromechanical coupling. This coupling is described below. The use of impedance to characterize the transducer performance follows the discussion of electromechanical coupling

C.1.1 Electromechanical Coupling

The study of electromechanical coupling looks at how the electrical and mechanical regimes interact when converting electrical energy into mechan-

ical energy. In an electromechanical system there are two inputs and two outputs that are coupled together inside the transducer. Using this analogy, the transducer is seen as a black box with the current and the velocity being the inputs and the electromotive force and impressed mechanical force as the outputs. Figure C.1 shows a schematic for an electromechanical transducer.

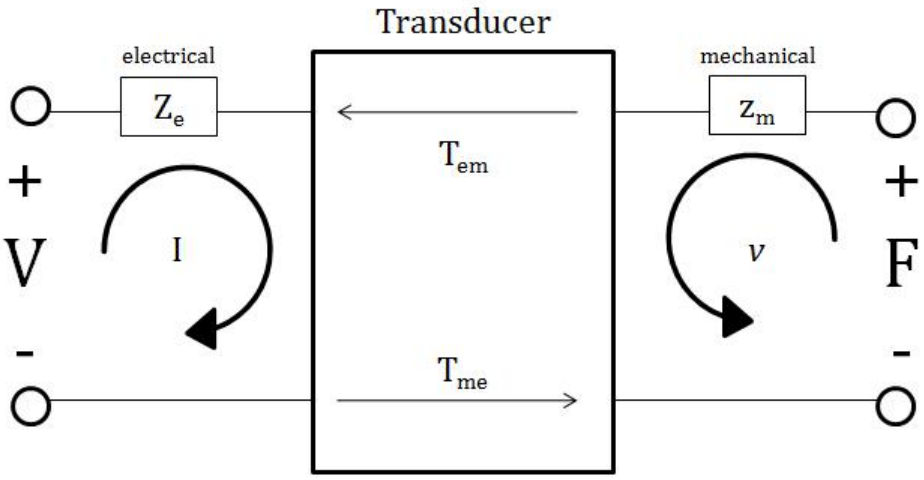

Figure C.1: Shematic Depiction of an Electromechanical Transducer

This leads to the two equations below where V is the voltage, Z_e is the electrical impedance, I is the current, T_{em} is the transduction coefficient converting mechanical to electrical energy, v is the velocity, F is the impressed mechanical force, T_{me} is the tranduction coefficient converting electrical to mechanical energy, and z_m is the mechanical impedance, [12]

$$V = Z_e I + T_{em} v, \tag{C.1}$$

$$F = T_{me} I + z_m v. \tag{C.2}$$

By looking at the symmetry of the system, it can be shown that the tansduction coefficients are equal in magnitude, and for a magnetostrictive material are opposite in sign. This implies that $T_{me} = -T_{em}$. This is an important observation in the study of electromechanical transducers and the coupling between the eletrical and mechanical regimes. These relationships are an important part of the impedance analyis described below.

C.1.2 Impedance Analysis

The impedance analysis of the circuit begins with setting the impressed mechanical force equal to zero. With this boundary condition, the transfer function between the terminal voltage, E, and the current, I, can be written as

$$\begin{aligned} Z_{ee} &= (\frac{E}{I})_{F=0} && \text{(C.3)} \\ &= \frac{Z_e z_m - T_{em}T_{me}}{z_m} && \text{(C.4)} \\ &= Z_e + \frac{-T_{em}T_{me}}{z_m}. && \text{(C.5)} \end{aligned}$$

The second term in this equation can be called the motional impedance. This reduces the equation to, [12]

$$Z_{ee} = Z_e + Z_{mot}. \qquad \text{(C.6)}$$

In this equation, Z_e is called the "blocked" impedance and Z_{ee} is known as the free, or total, impedance. The total impedance of the transducer can be measured over a wide range of frequencies using a stepped sine input and recording the complex transfer function. This transfer function will have a kinking shape as the freqeuncy of the input current goes through the resonant and anti-resonant frequencies. The blocked impedance can be found by looking at the real and imaginary parts of the total impedance and interpolating both the real and imaginary parts of the data separately at frequencies above and below the resonant frequency. For the impedance data, the real part represents the resistance value and the imaginary part is the reactance. Subtracting the blocked impedance from the total impedance results in the motional impedance. This data can be used to determine the resonant and anti-resonant frequencies as well as other characteristics of the transducer. This process and the resulting characteristics of the transducer tested in this research are discussed in further detail in the results and discussion section of this appendix.

C.2 Experimental Set Up

The testing set up for this set of experiments involves hanging the transducer from a frame to allow the Galfenol rod to experience free-free end conditions. The frame is constructed so that the transducer described in Chapter 2 can be hung from the edges and thus allow the rod to rest freely in the holes in the magnetic circuit. The frame is made of Unistrut members

with a threaded rod connecting the two sides. Fishing line is then strung around this rod and used to support the transducer. Figure C.2 shows the overall set up, and Figure C.3 shows a close up of the magnetostrictive transducer.

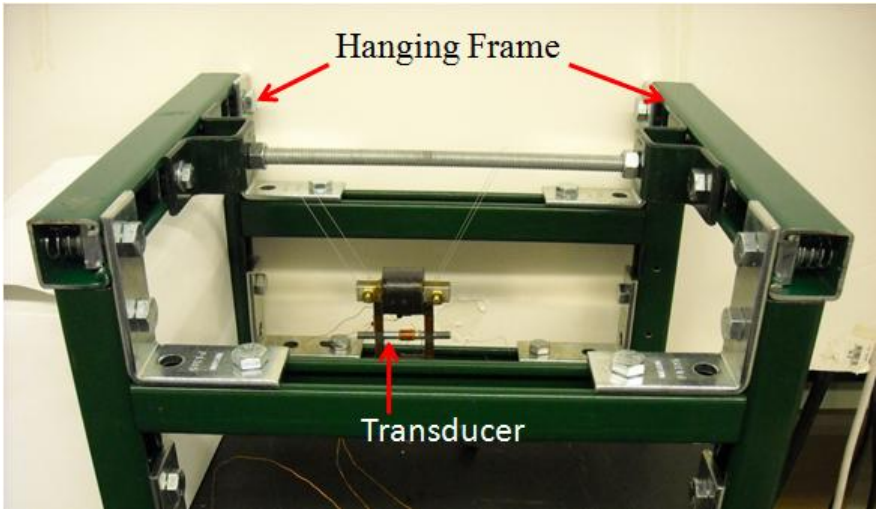

Figure C.2: Frame Structure for Hanging Transducer

To run the tests and analyze the impedance, the excitation coils of the transducer were connected to a AE TECHRON LVC 5050 Linear Amplifier. The amplifier was excited by a stepped sine signal from a Quattro Data Aquisition software. The test kept the amplitude of the current to the coils at 20 mA and adjusted the voltage accordingly. The current was measured using a Fluke i30s Current Clamp. The voltage from the pick-up coil was also fed into the Quattro, and the transfer function between this voltage and the input current recorded. The remainder of the alysis as described in the following section was performed offline using Matlab software.

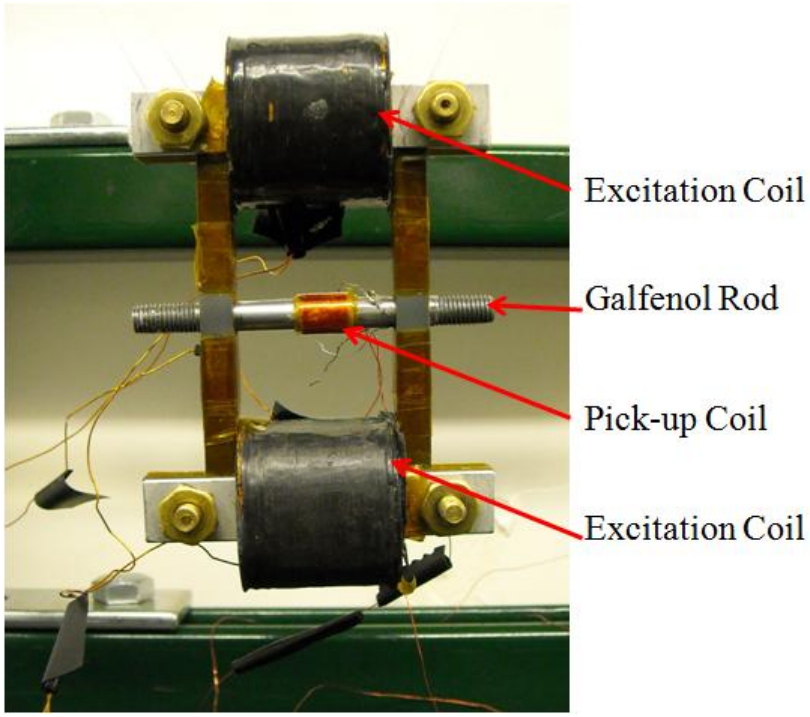

Figure C.3: Magnetostrictive Transducer Hanging from Frame

C.3 Results and Discussion

This section of the appendix looks at the analysis used to characterize the performance of the transducer. The first step in the characterization process is the determineation of the impedance and admittance transfer functions by using the stepped sine input. After determining these sets of data and some of the important quantities that are associated with each, the analysis can then move to looking at the damping present, the lag angle for the flux, and the electromechanical coupling.

C.3.1 Impedance and Admittance

Figure C.4 shows the magnitude of the electrical impedance transfer function under mechanically free conditions and Figure C.5 shows the phase. This data has been smoothed using a moving average function in Matlab to reduce the noise. The data below shows the kinking that was described earlier. For the transducer analyzed here, this occurs between 19 and 20 kHz. The blocked impedance was calculated as described above, and the specifics can be seen in Figure C.6. This figure shows the resistance and reactance, (R_{ee} and X_{ee} respectively), of the total impedance, and the resistance and reactance, (R_e and X_e respectively), of the blocked impedance.

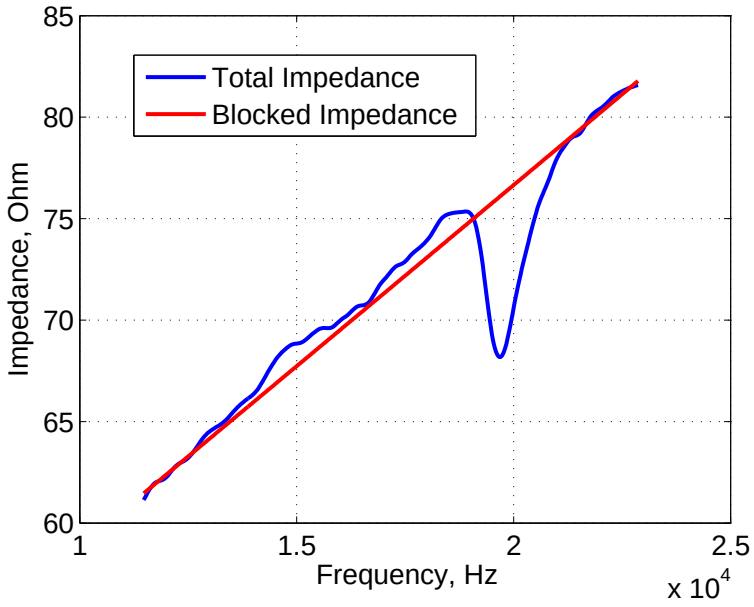

Figure C.4: Impedance Measurement of the Transducer

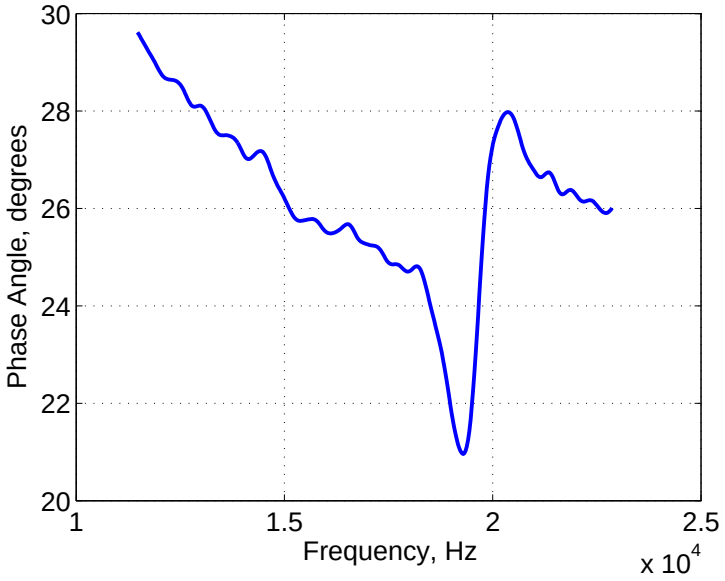

Figure C.5: Phase Angle of the Total Impedance

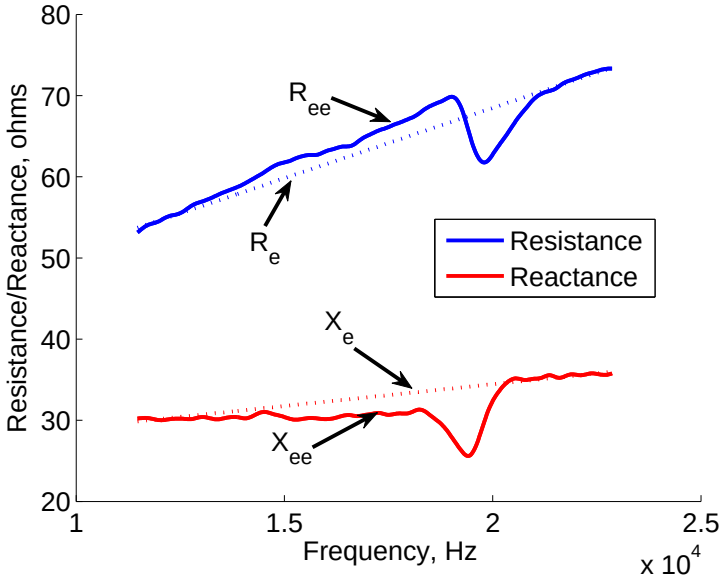

Figure C.6: Resistance and Reactance of Impedance Measurement

The motional impedance for this transducer was found using

$$R_{mot} = R_{ee} - R_e, \tag{C.7}$$

$$X_{mot} = X_{ee} - X_e. \tag{C.8}$$

This data was then plotted two show the reactance versus resistance. This graph is important because it can be used to characterize the performance of the transducer. The first characteristic that can be determined is the natural frequency. The natural frequency corresponds to the point on the diameter of the circle that crosses the origin. The value of the diameter can be used with further testing to detemrine the mechanical constants of the system. The quadrantal, or half-power, frequencies can also be found from this graph. The half-power frequencies are located at either end of the diameter that is perpendicular to the dimeter of the natural frequency, or principal diameter. The importance of these values will be discussed later in this section. The final characteristic that can be determined from the motional impedance circle is the lagging angle β. The amount that the principal diameter dips below the real axis is equivalent to 2β. This lagging angle, β, shows how much the induced magnetix flux lags behind the electromotive force. Figure C.7 shows the motional impedance circle obtained as a result of this experiment. The natural frequency (f_0), half power frequencis (f' and f"), and the depression angle (2β) are shown. [12]

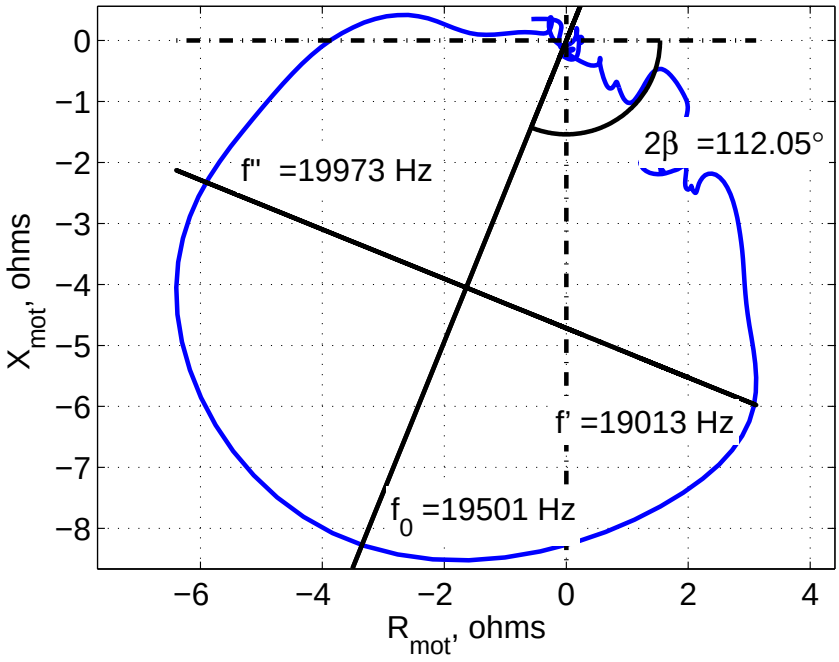

Figure C.7: Motional Impedance Circle

For further analysis the corresponding admittance diagrams were also plotted. The admittance is the reciprocal of the impedance; however, the motional admittance, (Y_{mot}), is not the reciprocal of the motional impedance. To determine the motional admittance, the total and the blocked admittance are first found as the reciprocal of the total and blocked impedances. The motional admittance is then given by, [12]

$$Y_{mot} = Y_{ee} - Y_e. \tag{C.9}$$

Figure C.8 shows magnitude for the total and blocked admittance and Figure C.9 shows the phase. Figure C.10 shows the motional admittance circle. From the motional admittance circle, the anti-resonant frequency can be determined in a similar manner to the resonant frequency. The half-power frequencies associated with the anti-resonant frequency can also be determined. Figure C.10 shows the motional admittance circle with these points labeled.

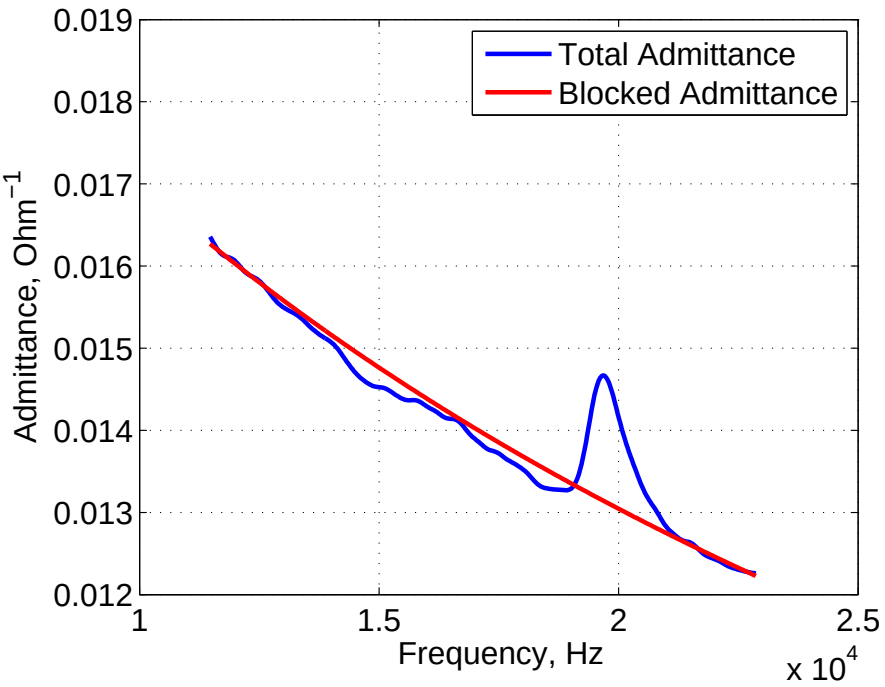

Figure C.8: Free and Blocked Admittance

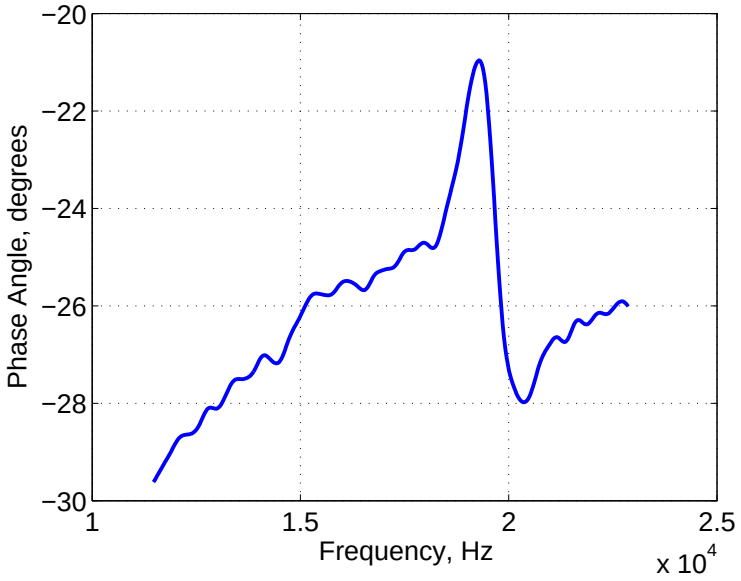

Figure C.9: Phase Angle of the Total Admittance

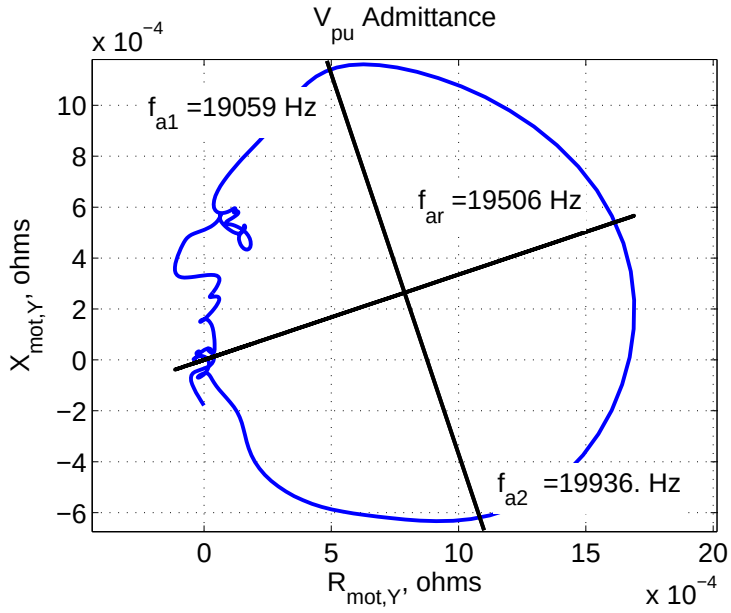

Figure C.10: Motional Admittance Circle

C.3.2 Damping

One of the characteristics of the transducer that can be determined from the data found in the motional impedance circle is the quality factor. The quality factor is related to the angle θ which is the deviation from the principal diameter as measured from the origin. This means that when θ is $\pm$ 45°, the corresponding points on the motional impedance circle are the half power frequencies. The relationship between the quality factor and this angle is, [12]

$$2Qp = tan\theta, \tag{C.10}$$

where,

$$p = \frac{1}{2}(\frac{\omega}{\omega_0} - \frac{\omega_0}{\omega}). \tag{C.11}$$

From this relationship it can be seen that when θ is $\pm$ 45°, the right side of the equation becomes $\pm$ 1 respectively. Solving for Q, adding these two equations, and combining the equations shown above the leads to,

$$\frac{\omega'\omega_0}{\omega'^2 - \omega_0^2} + \frac{\omega''\omega_0}{\omega''^2 - \omega_0^2} = 2Q. \tag{C.12}$$

Simplifying further, this equation can be reduced to a simpler relationship between the quality factor, Q, and the half power (ω' *and* ω") frequencies, and resonant frequency (ω_0). This relationship is given by,

$$Q = \frac{\omega_0}{\omega'' - \omega'}. \tag{C.13}$$

The damping ratio, ζ, of the system is given as $\frac{1}{2Q}$, and for this system was found to be 0.0246. This is equivalent to little damping in the system, and this knowledge can be used in further analysis of the transducer.

C.3.3 Flux Lag Angle

The angle β is the lag angle of the flux from the electromotive force. For an electromechanical transducer using a magnetostrictive element such as is the case in this thesis, this lag is caused by losses in eddy currents as well as hysteresis. [12] This angle is a property of the specific transducer and can have a wide range of values. For the transducer studied here, the lag angle was found to be approximately 56°. The motional impedance circle shows a depression angle of 2β becasue there are two components being taken into account. The first component is a lag in the electromotive behind the current with a lag angle of β_1. The second componenet is the lag of the flux, and thus voltage behind the induced electromotive force. This is given the angle β_2. In general, $\beta_1 \neq \beta_2$, but their difference is small and for practical analysis $\beta_1 + \beta_2 = 2\beta$ is used and the discrepency caused by the difference in the angle is ignored. [14]

C.3.4 Electromechanical Coupling

Another area that can be analyzed using the motional impedance and admittance circles is the electromechanical coupling. This relates how much of the electrical energy is transfered to the mechanical regime. In electromechanical tansducers, the frequency separation between the resonant and antiresonant frequencies serves as an indication of the effective coupling. This transducer shows an effective coupling coefficient, k_{eff}, of 0.022. For a transducer that uses a magnetostrictive element, this is called electromagnetic coupling and is given by,

$$k_{eff}^2 = 1 - (\frac{f_r}{f_{ar}})^2. \tag{C.14}$$

C.4 Conclusion

The impedance analysis of this transducer provided useful information about the performance of the transducer. This analysis determined the resonant frequency of the transducer as well as the damping present and the lag angle of the flux. The electromechanical coupling coefficient was also determined with respect to the transducer as a whole. This information is important in determining the performance, especially related to the frequency bandwidth. By determining where the resonant frequencies are and the different metrics of performance, this transducer can be better characterized for dynamic performance.

The research outlined in this appendix was a good step to understanding the performance of the system, and more work can be done to better understand the stransducer and the mechanical constants of the system. This entails doing a similar study with the transducer in a loaded state. In this study, the the magnetostrictive element would be loaded and the impedance analysis performed in a similar manner described in this appendix. The unloaded state was a first step in characterizing the dynamic perfomance of this transducer.